Differential Signal of Change Among Multiple Components of West African Rainfall

Omon Aigbovboise Obarein (oobarein@kent.edu)
University of Ibadan https://orcid.org/0000-0002-6702-1143
Cameron C. Lee
Kent State University

Research Article

Keywords: Rainfall variability and change, Tropical climate, West Africa

Posted Date: October 28th, 2021

DOI: https://doi.org/10.21203/rs.3.rs-825136/v1

Version of Record: A version of this preprint was published at Theoretical and Applied Climatology on April 21st, 2022. See the published version at https://doi.org/10.1007/s00704-022-04052-1.

Abstract

Rainfall components likely differ in the magnitude and direction of their long-term changes for any given location, and some rainfall components may carry a greater regional signal of change than rainfall totals. This study evaluates the magnitude of change of multiple rainfall components relative to other components, and the greatest regions of change across all rainfall components in West Africa. Hourly rainfall data from the ERA5 reanalysis dataset was used to derive twelve rainfall components, which were evaluated for long-term means, interannual variability, and long-term changes. For rainfall totals and rainfall intensity, the central Sahel is witnessing increasing trends while the western Sahel is experiencing significant decreasing trends. In general, decreasing trends predominate in the study domain, especially in the northwestern Congo Basin, where annual rainfall is decreasing by 120mm per decade. Importantly, rainfall frequency accounts for 49% of all significant grid-point trends for the whole domain. In contrast, rainfall totals account for 26% of all combined significant trends across the domain, while rainfall intensity (12.6%), rainy season length (9.5%), and seasonality (3.3%) account for the remaining signals of change. Most of the changes among the rainfall components are in the Tropical Wet and Dry regions (59% of all significant trends); the Saharan and Equatorial regions account for the least changes. This study finds evidence that rainfall frequency is changing more across the regions compared to rainfall totals and should be explored as rainfall inputs in climate models to potentially improve regional predictions of future rainfall.

I. Introduction

Studies of tropical climate variability and change have traditionally been carried out with a disproportional focus on rainfall totals (Trenberth et al., 2007; Feng et al., 2013) or other single rainfall 'components.' However, tropical rainfall can be disaggregated into a whole range of different components [e.g., rainfall frequency, intensity, timing, seasonality, zones, etc. (Table 1; Olaniran, 2002)], in addition to just totals, all of which may be impacted as a manifestation of global-scale climatic change. Analyzing rainfall totals is important in understanding seasonal rainfall distribution, but it is often a quick way of conceptualizing rainfall as a climate variable to permit easy regional comparison. Also, rainfall totals are the major rainfall parameters in climate models. However, since tropical rainfall can be disaggregated into several different components, the narrow focus on one of them does not provide a full picture of the potential changes to the tropical climate over the past four decades in response to both external forcing and internal climate variability.

Table 1
Definition of Rainfall components and indices

Rainfall components	Definition/derivation of Indices
Rainfall Totals	Daily totals (mm/day): summations of all the hourly rainfall for every 24 hours (beginning from 1979-01-01-07-00 UTC) for all 40 years. Annual totals (mm/year): summations all the daily rainfall within each calendar year for all 40 years. JJAS totals (mm/year): summations of all June, July, August, and September rainfall within each year for all 40 years.
Rainfall Frequency	Total rain-days frequency (days/year): All rain-days exceeding 0.25mm Light rain-days (days/year): The annual count of qualified rain-days (defined as those exceeding 0.25mm) with daily rainfall amounts at or below the 10th percentile of all qualified rain-days. Moderate rain-days (days/year): The annual count of qualified rain-days (defined as those exceeding 0.25mm) has daily rainfall amounts between the 10th and 90th percentile of all qualified rain-days. Heavy rain-days (days/year): The annual count of qualified rain-days (defined as those exceeding 0.25mm) with daily rainfall amounts at or above the 90th percentile of all qualified rain-days. Mean daily hours of rainfall (MDHR) per year (hr/yr): Daily rainfall hours summed for each year and averaged.
Rainfall Intensity	Rainfall Intensity (mm/yr): The ratio of the total annual rainfall to the annual number of days of rainfall.
Rainfall Timing	Defined using the mean cumulative rainfall method by Ilesanmi (1972): the mean annual rainfall (1979–2018) that occurs at each 5-day interval (a pentad) and expressing each pentad rainfall as a percentage of the total annual rainfall. This percentage is cumulated for each year and across grid-points. Onset (Julian days): The 8% cumulated rainfall Cessation (Julian days): The 90% cumulated rainfall Rainy season length (RSL) (Julian days): the intervening days between the onset and cessation dates
Rainfall Seasonality	Seasonality Index (SI): The sum of the absolute deviations of mean monthly rainfalls from the overall monthly mean, divided by the mean annual rainfall (Walsh & Lawler, 1981).

The IPCC (Stocker et al., 2014) reported that there was no significant trend in total tropical rainfall for the 1901–2008 and 1951–2008 period because decreasing trends in the 1970s – 1990s had been offset by increasing trends in the last couple of decades (Trewin, 2014), especially in the Sahel. It then becomes pertinent to ask: Is this outcome peculiar to rainfall totals alone, or have other rainfall components shown similar trends? In what ways have other rainfall components (besides rainfall totals) changed in the studied period? Without considering other rainfall components, we risk missing aspects of the changing tropical rainfall that might even be more important than totals. More importantly, the responses of many systems are more critically impacted by these other rainfall components. For example, the timing of rainfall is more crucial to West Africa's rain-fed agricultural sector than rainfall totals (Obarein & Amanambu, 2019; Adefolalu, 1986), and the frequency and intensity of rainfall have a greater influence on floods than rainfall totals.

Further, there is some evidence in the literature that rainfall totals are often less sensitive to climate variability compared to other rainfall components (e.g., Alpert et al., 2002), and any two rainfall components may show different trends (in both direction and magnitude) for the same location and period (Lodoun et al., 2013). Therefore, it is likely that other rainfall components are more sensitive (or at least differ in their respective sensitivities) to climate variability and change than rainfall totals. These relative climate sensitivities have not been explicitly investigated. Detailed estimates

of past tropical rainfall changes and accurate projections of future tropical rainfall changes should be cognizant of all disaggregated tropical rainfall components, without which such projections will be incomplete.

This study, therefore, sought to evaluate the magnitude of change of each disaggregated rainfall component relative to all other components, and the locations of greatest change across all the different rainfall components in West Africa. This study also explores ENSO teleconnection with the aforementioned rainfall components because, while the lagged impact of ENSO on West African rainfall is well documented, this teleconnection has been mostly linked to rainfall totals.

The choice of West Africa is not arbitrary because its many rainfall regions are arguably more representative of tropics-wide conditions than most tropical sub-regions and thus ideal for this study. Also, West Africa is one of the most vulnerable regions to climate change-induced rainfall extremes (Aryeetey-Attoh, 1997; Niang et al., 2014; Yaro & Hesselberg, 2016). The Sahel, in particular, continues to be the focus of research in tropical rainfall climatology because of its sensitivity to substantial multi-decadal variability (Akinsanola & Zhou, 2019b; Mohino et al., 2011; Owusu & Waylen, 2009; Mahe et al., 2001). The Sahelian drought of the 1970s and 1980s, which was largely responsible for the reduction in global land precipitation (Dore, 2005), was preceded by the wet decades of the 1950s and 1960s (Bichet & Diedhiou, 2018), and followed by the recovery in the 1990s. Current estimates of future West African rainfall—mostly of rainfall totals—is uncertain (Monerie et al., 2020; Sylla et al., 2016; Niang et al., 2014). Therefore, by unearthing evidence of a higher signal of rainfall change in other rainfall components (besides rainfall totals), the case can be made for including that in future estimates of West African rainfall.

Ii. Data And Methods

The study domain covers West Africa (Fig. 1). The domain stretches from 1°N – 21°N and 21°W – 18°E, but with analyses performed on land-based grid-points over West Africa. Hourly rainfall from the ERA5 gridded reanalysis dataset developed by the European Centre for Medium-Range Weather Forecasts (ECMWF; Hoffmann et al., 2019) was used to derive the rainfall components/indices used in this study. The dataset has a spatial resolution of 0.25^{o} x 0.25^{o} and covers the period 1979 to 2018. Reanalysis numerical weather prediction (NWP) models are fed by many familiar sources of observational climate data (such as ground-based stations, weather ships, radiosondes, and weather satellites). However, the ERA5 reanalysis is greatly improved through its assimilation of observations from the Advanced Scatterometer (ASCAT), the Microwave Humidity Sounder (MWHS), and many other recent sophisticated weather satellite instruments (Dee & NCAR, 2020; Dee et al., 2016). This improved data assimilation capacity explains why the ERA5 has a better spatial and temporal resolution and has more parameters than the ERA-Interim (Hoffmann et al., 2019; Urraca et al., 2018; Olauson, 2018).

2.1 – Estimating Long-term trends and variability

The method of derivation for each rainfall component is summarized in Table 1. The long-term variability of each of the indices was evaluated using the median absolute deviation (MAD) statistic. The MAD is computed by first finding the median, then calculating the absolute deviations from the median, and computing the median of these absolute deviations. The commonly used standard deviation statistic is problematic because both the standard deviation and the mean are sensitive to outliers. MAD has been shown to circumvent this problem and is ideal for estimating statistical dispersion in a climatic time series (Leys et al., 2013; Kwak & Kim, 2017).

At each grid point, long-term trend detection was done using the Theil-Sen slope estimator. It is a method for fitting a line to a set of points that chooses the median slope among all lines connecting all possible pairs of two-dimensional sample points (Sen, 1968; Theil, 1950). It is insensitive to outliers and is more robust than the simple linear regression

method of least squares, especially in datasets that are not normally distributed (Ohlson and Kim, 2015). The Theil-Sen estimator is becoming more popular in detecting monotonic trends in univariate time series, such as climatic datasets.

Statistical significance of trends was estimated using 1000 bootstrap resamples of the Theil-Sen slope estimation to derive 95% confidence intervals. Confidence intervals were calculated based on MATLAB's bias-corrected accelerated percentile method and converted to p-values using the technique outlined in Altman and Bland (2011). To tackle potential misinterpretation of statistical significance arising from multiple statistical tests at many spatially autocorrelated grid points, we controlled for the false detection ratio (FDR) as suggested by Wilks (2016). Since bootstrapping and Theil-Sen are quite computationally expensive, simple linear regression was used to save computational time in computing daily-level rainfall trend estimates. To visualize decadal-scale changes in rainfall components, the Theil-Sen slope estimates have been multiplied by 9 (n-1; where n is 10, the number of years in a decade).

2.2 – Estimating relative changes using standardized z-score values

To better quantify the magnitude of change of each rainfall component relative to other components (i.e., to examine which rainfall components are changing the most and where), we must transform the slopes (at each grid-point for all rainfall indices) into equivalent units. A modified 'robust' Z score formula (Eq. 2) was used (see Choudhury et al., 2017 and Srivastava, 2017), which simply replaces the mean and standard deviation in the well-known standardization procedure (Eq. 1) with the median slope value and MAD of the set of slopes (across space) for each rainfall component, respectively. Since the aim is to quantify the spatial distribution of relative changes (i.e., relative to the other components), the sign of Z is less important (and potentially misleading) than the absolute values of Z—which were thus used in the results below.

$$Z = \frac{x - \bar{x}}{S}; \quad (1)$$

Where x, $\bar{x}$, and s are the sample, sample mean, and sample standard deviation respectively

$$Z = \frac{x - M}{MAD}; \quad (2)$$

Where x, M, and MAD are the slope values, median slope value, and MAD, respectively.

Relative changes were also quantified by summing the count of all significant grid-point trends in each rainfall component.

2.3 – Relationship with ENSO

The time series of the different rainfall components were analyzed for associations with ENSO signals. To evaluate possible ENSO signals on each tropical rainfall component, first, NOAA's Oceanic Niño Index (ONI) (which is NOAA's primary indicator for monitoring ENSO [Dahlman, 2016]) is used to quantify ENSO activity. The ONI is a 3-month moving average SST anomaly for the Niño 3.4 region. An annual ONI was computed that classifies each season into one of three groups: Neutral event, La Nina event, or El Niño event (Supplementary material, Table S1). Based on NOAA's operational definition of the ONI, a year was designated an El Niño year if it has five consecutive 3-month moving average SST anomalies at or above + 0.5°C. A La Nina year would be one with five consecutive 3-month moving average SST anomalies at or below − 0.5°C. A neutral year does not satisfy these conditions. The annual ONI was computed by averaging all 3-month moving average SST anomalies in each ENSO season, starting in the boreal winter.

Typically, ENSO-rainfall teleconnection is investigated by making the ENSO indices lag rainfall indices by 3–9 months (e.g., Xu et al., 2004; Manatsa et al., 2017; Lee et al., 2020, among others). Wang et al. (2020) and Camargo and Sobel (2005) found that a lag time of six months produced the strongest correlation between ENSO and SSTAs in the Bohai Sea and the Yellow Sea, and between ENSO and tropical cyclone activities, respectively. However, because the situation may be different for West Africa, this research correlated rainfall indices with the annual ONI of each ENSO season, using the Pearson's moment correlation coefficient, r, effectively minimizing any significant difference in correlation arising from using different lag times. P-values were calculated from the correlation coefficients to test the hypothesis of no correlation against the alternative hypothesis of a non-zero correlation (with $\alpha = 0.05$).

2.4 – Rainfall Regionalization

Theoretically, rainfall zones—regions of homogenous rainfall characteristics—can be defined using any one of the tropical rainfall components. However, only rainfall totals are used to determine rainfall zones herein to stay within the convention and avoid unnecessary complexity. The main rainfall regions were defined using k-means based regionalization of the entire 40-year dataset. This method begins by placing a predetermined number of k centroids randomly in space, based on the number of clusters required. The next step involves computing the distance between each grid-point and a centroid and assigning a grid-point to the closest centroid. This first iteration creates k number of clusters, but on the next iteration, the centroids shift to occupy a new position in space based on the average of all the members in the cluster. Some grid-points may change clusters if it becomes closest to a new centroid as a cluster centroid shift. Iterations are performed until no grid-point changes cluster membership (Hannachi, 2004; Carvalho et al., 2016). K-means was applied to the 12 averaged (over 40 years) monthly mean rainfall amounts for each of the 9066 grid-points, and each grid-point was classified into one of 5 clusters/regions.

No consistent standard zonation of West African rainfall exists in the literature. Cluster evaluation metrics yielded varying results, so five clusters were chosen, as this solution yielded five rainfall zones, with distinctive mean annual rainfall totals, mean monthly totals, and mean annual regimes (Fig. 2). Cluster 1 and 5, representing the Sahara Desert zone and the rainy equatorial southern coastal zone, respectively, have the most contrasting rainfall characteristics and are two of the most easily recognizable rainfall zones. The Sahelian zone (cluster 4) has received considerable attention because of its well-documented multi-decadal rainfall oscillations and fragile environment (Dong & Sutton, 2015; Giannini et al., 2013; Bichet & Diedhiou, 2018). As cluster 4 shows, most of the rainfall in this zone occurs in the boreal summer, with a peak in August (Nicholson et al., 2018). Cluster 2 and 3 have also featured prominently in previous literature as the other three regions described above, with the terms' Guinean' and 'Sudanian' used to describe them, respectively (Akumaga & Tarhule, 2018, Camberlin et al., 2020), possibly due to the vegetation class in these regions. Cluster 2 is closer to the equatorial zone and so receives more total rainfall than cluster 3, whose northern boundary is the Sahelian zone. However, the most contrasting feature of these two regions is their annual cycle, clearly depicted in Fig. 2a. The Tropical Wet region (cluster 2) has a bimodal annual rainfall distribution because the ITCZ makes two overhead migrations as it moves northward and southward during the West African Monsoon (Diallo et al., 2016). By contrast, the Tropical Dry region (cluster 3) has a unimodal annual rainfall distribution (Nkrumah et al., 2019). In all, these five clusters capture most of the known spatial variability in total rainfall characteristics across West Africa.

2.5 – Validating the ERA5 precipitation dataset

For all the benefit of reanalyses datasets, legitimate concern exists in the climate science community about the accuracy with which reanalysis datasets reproduce atmospheric variables, especially precipitation, on local to regional scales. There are also concerns about the use of reanalysis data for trend analysis. However, reanalysis data are the only source of complete long-term data at regular temporal and spatial intervals in West Africa and other regions of the world that suffer from a sparse network of ground-based observations. Reanalyses are a necessity for many climate studies in

these areas. In all the evaluations of the ERA5 reanalysis reviewed for this research, ERA5 outperformed previous reanalysis products (see Zhang et al., 2019; Delhasse et al., 2019, and Mahto & Mishra, 2019). And although validations of ERA5 precipitation data for Africa relative to the Climate Hazards Group InfraRed Precipitation with Stations version 2 (CHIRPS v2) yielded significant improvements over ERA-Interim (Gleixner et al., 2020), no such validations exist for the West African region specifically. In this section, the ERA5 precipitation data is validated against a diverse set of precipitation products: ground observation weather stations (the full list of stations is in Supplementary Table S2), Tropical Rainfall Measuring Mission (TRMM) data, and Tropical Applications of Meteorology using Satellite and ground-based observations (TAMSAT) data. Information on time span, spatial resolution, and data repository are summarized in Table 6. All validation data are monthly rainfall totals. The ERA5 data, which is monthly averaged precipitation, was resampled to the grid size of each validation data to facilitate grid-by-grid validation of raw data. Mean monthly precipitation and precipitation variability were also evaluated but over the entire study area. The MAD was used to measure variability, and all validation was done by correlating both sets of data with the Pearson product-moment correlation coefficient.

Table 6
Precipitation datasets for ERA5 validation.

Precipitation dataset	Component products	Data repository/Sources/Citation	Time period	Grid sizes (spatial resolution)
TAMSAT	Satellite-derived data	Maidment et al. (2017); Tarnavsky et al. (2014); Maidment et al. (2014)	1983–2020	0.0375–0.0375
TRMM	Satellite-derived data	EarthData GIOVANNI	1998–2015	0.5^{o} x 0.5^{o}
Ground observation station	Ground stations	Nigerian Meteorological Agency (NIMET)	1982–2011	NA

Iii. Results And Discussion

The results and discussion section will focus on the unique rainfall components and indices out of the 13 that were evaluated. The long-term means, variability, and trends of all indices are shown in Supplementary Figures S1, S2, S3, and S4, respectively. Supplementary Table S3 and S4 presents a breakdown of regional trends for all 13 indices as decadal changes and average percentages. Finally, Supplementary Tables S5 and S6 show the regional percentage of grid-point trends for all rainfall indices and ENSO association with all rainfall indices.

Daily, annual, and JJAS rainfall totals show very similar long-term means and trends. All rainfall frequency indices have similar long-term means, with moderate rainfall and total rain-days having similar long-term patterns. The rainy season length (RSL) is a function of the onset and cessation of rainfall. Therefore, this study will focus primarily on five rainfall components/indices: annual rainfall, total rainfall days, rainfall intensity, rainfall seasonality, and rainy season length.

3.1 – Long-term means of Rainfall Components

There is an observable latitudinal variation in long-term means across all rainfall components in the study domain (Fig. 3). Total rain-days and rainfall seasonality (Fig. 3b & 3d) surprisingly show more glaring latitudinal rainfall distribution than rainfall totals and rainy-season length (RSL) (Fig. 3a & 3e), which have been traditionally used to describe the latitudinal distribution of the West African rainfall regime (e.g., Hagos & Cook, 2007; Trewin, 2014). The strength of the latitudinal distribution in rainfall frequency and seasonality is seen in the continuous east-west band of rainfall characteristics. Unlike rainfall totals, rainfall frequency and seasonality appear insensitive to localized increases in rainfall in high elevation areas. The latitudinal discontinuity in the distribution of total rainfall and RSL is seen in

highland areas and primarily at the coast where relative dryness occurs—which breaks the coastal band of heavy rainfall between the coast of Cameroon through the Niger Delta to the coast of Liberia and Sierra Leone, where mean annual rainfall is at least 3000mm.

Still, the latitudinal distribution of rainfall totals is a prominent feature of West African climate and tropical climates found, to varying degrees, elsewhere, such as central Africa and the Indonesian/Australian region (Trewin, 2004). This feature involves a transition from the heaviest rainfall zone, outside the equator, to a vast zone of relatively lesser rainfall and then to a dry zone—often a desert. The rainy coastal zone of West Africa occurs near 4–5°N latitude, and from this zone, rainfall decreases with distance away from the coast, northward up to the Saharan region.

Unlike rainfall totals and RSL, there is little reference to rainfall frequency and seasonality as rainfall components that exhibit a precise latitudinal distribution. The earliest attempts at regionalizing West African rainfall only considered rainfall totals and RSL (Nicholson, 1979, 1980, 1993. This contrast in capturing localized rainfall disparities gives an insight into the climatological difference and similarity between rainfall totals on the one hand (Fig. 3a) and rainfall frequency and seasonality (Fig. 3b & 3d), on the other. It is possible that, in failing to capture localized orographic rainfall, rainfall frequency, and seasonality heavily reflect mid-tropospheric rainfall mechanisms that drive the development of mesoscale convective systems (MCSs), and thus of rainfall (Akinsanola & Zhou, 2019; Nicholson, 2009; Cretat et al., 2015). Statistically and visually, total rain-days appear slightly independent of rainfall totals because more rainfall occurrences do not always translate into more rainfall totals: the correlation between spatially averaged mean annual rainfall and rain-days is 0.688.

North of 15°N, there is an almost total spatial uniformity in mean distribution among the rainfall components because of the extensively dry expanse of the Sahara Desert. With a mean annual rainfall total of less than 3mm, parts of the Sahara are the driest places on Earth (Kelley, 2014; Ghoneim & El-Baz, 2020). RSL, rainfall frequency, and rainfall intensity are also the least in this region, and the rainfall here is very seasonal because it is limited to 1–2 boreal summer months.

3.2 – Interannual Variability in Rainfall Components

Rainfall in dry tropical areas is marked by high interannual variability (relative to the mean) compared to wetter parts of the tropics where the higher rainfall tends to be more reliable (Nieuwolt, 1982; Ayoade, 2004). Figure 4 displays the spatial pattern of normalized interannual variabilities among West African rainfall components. To calculate this, the MADs are divided by the averages of the rainfall component for each grid point. The MADs are normalized because the spatial distribution of MADs is skewed by those grid points with higher values of rainfall characteristics.

The most variability is in the dry Sahara Desert, particularly the eastern portion, the driest in West Africa. From the Sahara, interannual variation in rainfall totals, rainfall frequency, rainfall intensity, and rainfall seasonality decreases, almost latitudinally, southwards to the coast. Rainfall intensity (Fig. 4c) displays the most latitudinal, north-south decrease in rainfall variation, while rainfall seasonality (Fig. 4d) displays the least latitudinal variation. In contrast to long-term means, the interannual variability in rainfall frequency and intensity south of 15^{o}N appears constant, compared to the dry north, where there is more considerable variation.

In general, interannual variability in West Africa is higher than interannual trends and even decadal trends for all rainfall components (Supplementary Figure S3). Globally, twentieth-century decadal trends in rainfall totals also tend to be lower than interannual variability (New et al., 2001).

3.3 – Regionalization of Rainfall Totals in West Africa

Figure 2b shows the result of the K-means cluster analysis of rainfall totals over the study domain for the 40 years of the study. Five distinct rainfall regions have been produced, based on the mean monthly rainfall of each grid-point. These five regions capture almost all the spatial variability observed over the decades in this region. The regionalization also captured the whole spectrum of the mean annual rainfall cycle (Fig. 2a) characteristic of West Africa. For all regions, the peak of the WAM is in the boreal summer that lasts from June to September.

In addition to the latitudinal distribution of the rainfall regions, the regionalization also depicts the necessary zonal discontinuity that captures the actual spatial variation of the rainfall regime in West Africa. Only the Saharan, Sahelian, and Tropical Dry regions stretch unbroken from east to west. Still, longitudinal bands of more homogenous rainfall characteristics have been identified in these regions, as seen in previous research (Nicholson, 1993; Klutse et al., 2016). In all, the drier, northern rainfall regions are more spatially contiguous than the wetter, southern regions. A tabulation of some rainfall characteristics in each rainfall region is presented in Table 2.

Table 2
Summary of selected rainfall characteristics for each rainfall region (1979–2018).

Rainfall Characteristics	Saharan	Tropical Wet	Tropical Dry	Sahelian	Equatorial
Mean altitude (m)	355	383	355	294	552
Max altitude (m)	2988	1231	1889	1350	2943
Mean annual rainfall (mm)	80	1648	1183	575	2557
Mean number of light rains (days)	3	31	19	13	28
Mean number of moderate rains (days)	26	252	156	100	222
Mean number of heavy rains (days)	3	31	19	13	28
Mean number of rain-days (days)	32	314	194	126	278
Mean Onset (dates)	June 3	March 6	May 3	June 2	Apr 10
Mean Cessation (dates)	Sep 11	Oct 31	Sep 29	Sep 17	Oct 17
Mean RSL (days)	99	239	149	106	189
Mean Seasonality	1.4	0.4	0.9	1.1	0.6
Mean annual rainfall Intensity (mm/day)	1.97	5.23	6.17	4.59	9.34

3.4 – Long-term changes in Rainfall Components

The long-term changes in rainfall components are mapped as decadal changes in Fig. 5. Regionally-averaged decadal changes for each rainfall component are summarized in Table 3. Perhaps one of the most consistent and clearest signals of long-term changes among West African rainfall components is the contrasting trend between the central and western Sahel for annual rainfall totals (Fig. 5a) and rainfall intensity (Fig. 5c). Previous studies have reported this zonal contrast (e.g., Libel & Ali, 2009; Nicholson et al., 2018; among others). On average, annual rainfall totals are increasing by 40mm per decade in the central Sahel and decreasing by 120mm per decade in the western Sahel—these decreases are statistically significant.

Table 3
Decadal changes in rainfall indices subdivided by region. Statistically significant ($p < 0.05$) trends are underlined and in bold font. Shades of blue and red mark decreasing and increasing trends, respectively.

Rainfall components	Indices	Saharan	Tropical Wet	Tropical Dry	Sahelian	Equatorial
Rainfall total	Annual rainfall (mm/decade)	-0.116	-79.870	-49.690	16.480	-46.150
Rainfall frequency	Total rain-days (days/decade)	-0.388	-4.606	-4.615	-4.102	-1.782
Rainfall Intensity	Rainfall intensity (mm/day/decade)	0.018	-0.1827	-0.1152	0.0144	-0.1521
Rainfall seasonality	Rainfall seasonality	0.016	-0.003	-0.010	0.008	-0.002
RSL	RSL (days/decade)	-3.899	-3.223	-2.830	-4.528	-2.23

Very little research has sought to proffer an explanation for these contrasting trends in western and central Sahelian rainfall totals. Recently, Erfanian et al. (2016) found that a dynamic vegetation can lead to stronger effects of climate change on precipitation through a vegetation—precipitation feedback. Wang et al. (2017), incorporating land-use changes into regional climate models, found that climate-change-induced changes in crop yield impact precipitation, evapotranspiration, and soil moisture in the western Sahel and central Sahel. This linkage between climate change and the zonal contrast in Sahelian rainfall is further reinforced by Monerie et al.'s (2020) study, where a higher emission scenario strengthened the zonal contrast in the future period (2060–2099) over the historical period (1960–1999). Accounting for only internal climate variability, they found that the zonal contrast is associated with northern African surface warming and sea-surface temperature anomalies in the Pacific and tropical Atlantic oceans. In Getani et al. (2017), forcing the CMIP5 with higher CO_2 concentrations produces wetness in the Sahel, but with a stronger response in the central Sahel, whereas SST warming produces dryness in the Sahel, with a stronger response in the western Sahel. These two competing and contradictory responses may collectively (rather than individually) account for the observed zonal contrast in Sahelian rainfall trends.

The literature provides some evidence about the likely time when the central/western Sahelian rainfall trends contrast began to occur. The year 1994 was reported as the wettest year in the Sahel since the drought began in the 1970s (Nicholson et al., 1996; LeCompte et al., 1994), and Nicholson et al. (1996) found that most of those positive rainfall anomalies occurred in the central Sahel, with little increases in the western Sahel. In addition, these spatial anomalies were limited to the boreal summer and continue to drive the increases in central Sahelian rainfall, in agreement with Nicholson et al. (1996), Sanogo et al. (2015) and Biasutti (2013). Vegetative data analysis by Anyamba and Tucker (2005) also explicitly puts the start of the recovery of Sahelian rainfall in 1994, given the uptick in vegetation in that year. The contrasting trends between the western and central Sahel for annual rainfall totals and summer rainfall have likely grown stronger over time, and some studies now predict that it would persist to the end of the 21st century (Monerie et al., 2017).

The increasing trend in the Guinea coast and other coastal regions (for rainfall totals, intensity, and seasonality; Fig. 5a, c, & d) is surprisingly not experienced in other highland areas that make up the Equatorial zone. This difference suggests that increasing trends in these coastal areas may be feedbacks from a warming adjacent ocean, as precipitation is sensitive to local SST changes (He et al., 2018; Balas et al., 2007). Nicholson et al. (2018) and Jin & Huo (2018) have found that the Guinea coast of West Africa showed a very high correlation between rainfall and local SSTs in the JAS season for the 1969–2014 period compared to other coastal areas.

Furthermore, widespread decreasing trends exist across all rainfall components. One area of concern is the northwestern Congo Basin, experiencing significant decreases in rainfall totals, intensity, and seasonality (Fig. 5a, c, & d). Annual rainfall in the northwestern Congo Basin is decreasing at 120mm per decade, and total rain-days are decreasing by up to 2% (relative to their mean) per decade. The rainfall decline in the world's second-largest rainforest is well documented from empirical data on long-term rainfall totals (Malhi & Wright, 2004; Asefi-Najafabady & Saatchi, 2013; Hua et al., 2016; Jiang et al., 2019; and others), and observations of rainforest greenness (Zhou et al., 2014). Warm air masses in tropical regions have become more frequent, in lockstep with increases in air temperatures (Lee, 2020), but the increased absolute water vapor content of humid air has not led to increased rainfall in the Congo Basin and in many tropical rainforests (Malhi & Wright, 2004). Other studies have also noted decreasing trends in cloud cover in the Congo Basin (Lee, 2020), which may also contribute to declines in precipitation.

Jiang et al. (2019) and Zhou et al. (2014) have drawn attention to the observed massive intensification of the dry season, which has potentially created a positive feedback loop of vegetation drying and drought. Long-term drying can increase the land evaporative demand, reduce cloud cover, and increase aridity; and the deforestation in the Congo Basin only helps amplify the drying (Nogherotto et al., 2013). This study finds evidence of increased dry season duration in the shrinking of the RSL (by ten days per decade [Figure 5e]).

The widespread decreasing trend in rainfall totals and rainfall frequency in West Africa may be part of a larger drying signal in tropical land areas, particularly in the northern hemisphere tropics where this study domain lies (Neelim et al., 2006; Zhang et al., 2007). Malhi & Wright (2004) have reported precipitation declines in tropical rainforest regions, mainly driven by anthropogenic forcings—mostly logging and agricultural clearing. Attribution science in tropical rainfall changes is still somewhat fuzzy, and there is some consensus about the cause of the drying in the tropics; however, it is possible that the role of natural forcings or internal climate variability—such as SST anomalies and ENSO—have become relatively less prominent, especially in the last few decades as anthropogenic influences have become stronger (IPCC, 2021). Still, the oceans play a crucial role in modulating tropical rainfall and even causing sustained summer drying over land. For example, Hua et al. (2016) reported that Indo-pacific SST teleconnection with central African rainfall was the likely cause of the drying in the Congo Basin. The Congo Basin, regardless of the absence of any consensus on its drying, remains a major convection hotspot that influences regional climate by modulating the energy balance and hydrological cycle, and its future change will have significant regional climatic implications.

Importantly, the large-scale drying in the tropics seems to contradict the widely held paradigm that dry areas will get drier and wet areas will get wetter. Chadwick et al. (2013), Greve et al. (2014; [1948–2005]), and (Feng & Zhang, 2015 [1979–2013]) found that a robust 'dry gets drier and wet gets wetter' pattern occurred in only 10.8% and 15.12% of global land areas respectively: the vast portion of humid tropical Africa, especially the Congo Basin and the majority of the West African domain, are getting drier. The 'dry gets drier and wet gets wetter' pattern is more applicable to patterns of precipitation trends over the ocean (Hu et al., 2019; Greve et al., 2014); it is unlikely that land surfaces will follow a simplistic climate change pattern given the complex land-vegetation-climate feedback system, some of which have been mentioned above.

As mentioned above, RSL is shrinking, driven by delayed onset and earlier-than-normal cessation (Supplementary Figure S4). The delayed onset of the rainfall is consistent with African-wide trends reported in Dunning et al. (2018). The RSL is generally more dependent on the onset than on the cessation (Obarein & Amanambu, 2019), and a strong correlation between the former and the latter has been reported in some studies in Africa (Kanemasu et al. 1990; Mubuvma, 2013; Mugalavai 2008). This interdependency explains why a delayed onset is observed with a shorter rainy season in West Africa.

Averaged by rainfall regions (Table 3), most of the trends are negative and statistically significant, an unsurprising result given the broad swaths of statistically significant decreasing trends across the study domain in most rainfall indices. Areas of increasing trends are too localized to sway the general regional trend away from more widespread decreases in rainfall components. It is noteworthy that the Saharan region has no statistically significant trend for any rainfall components. Oppositely, the Tropical Dry and Wet regions are seeing the most significant trends.

Overall, the rainy south has witnessed more changes than the dry north. The trends in rainfall totals and rainfall frequency are broadly corroborated by the IPCC's (Niang et al., 2014) estimates: statistically significant decreasing trends in most of the domain and non-statistically significant increasing trends mainly in the central Sahel and the Guinea Coast. The IPCC projects that extreme rainfall days will increase by the end of the century, but the projections are low to medium confidence.

3.5– Relative Magnitude and Spatial Patterns of Changes among Rainfall Components

The relative changes in all rainfall components/indices, estimated by taking the absolute z-scores of the trends, are shown in Fig. 6. Another measure of the relative magnitude of changes among the rainfall components is the percentage count of total significant trends (on a grid-point basis) in each rainfall component, subdivided by region (Table 4 & Fig. 7). Both analyses show that the rainfall frequency (measured by total rain-days) has witnessed the greatest significant changes, accounting for almost 50% of all combined significant trends, relative to the other four components. Annual rainfall totals is the second greatest category of changing rainfall components (Fig. 6b), accounting for 26% of total significant trends. In contrast, RSL (9.5%), rainfall intensity (12.6%), and rainfall seasonality (3.3%) account for the least changes among the rainfall components in the last 40 years (Fig. 6l, h, & l; Table 4).

Table 4
Percentage of the total significant grid-points (trends) for rainfall indices in each region. The two highest percentages and the two lowest percentages are in red, bold font and blue, bold font, respectively.

Rainfall components	Indices	Saharan	Tropical Wet	Tropical Dry	Sahelian	Equatorial	Total count of Significant trends	% of total significant trends
Rainfall Totals	Annual rainfall	**6.5**	**31.4**	**39.0**	11.5	**11.4**	1837	25.6
Rainfall Frequency	Total rain-days	**17.4**	19.7	**29.7**	**30.8**	**2.4**	**3507**	**48.9**
Rainfall Intensity	Rainfall intensity	**2.9**	**50.6**	**24.9**	**1.9**	19.8	905	12.6
Rainfall Seasonality	Seasonality	**5.0**	14.6	**48.3**	**0**	**32.1**	240	3.3
RSL	RSL	**10.7**	18.1	**20.4**	**47.1**	**3.7**	680	9.5
% of total significant trends		**12**	28	**31**	**21**	**8**	7169	100

Changes in moderate rainfall, total rain-days, and MDHR per year account for the greatest regional rainfall change signal in the study domain. These changes are mostly in the Tropical Wet and Tropical Dry regions and in parts of the western Sahel (Fig. 7).

This finding is well supported by studies that have compared changes in rainfall frequency and rainfall intensity. Camberlin et al. (2009) and Moron et al. (2006), in their studies of East African and West African rainfall, respectively, found that rainfall frequency (total rain-days in particular) has the greater influence over regional-scale signals of interannual rainfall variability than rainfall intensity.

Figure 8 maps the total number of statistically significant trends across all rainfall components for each grid-point. In general, the south has undergone the bigger magnitude of change in the last 40 years compared to the north. In the south, two areas with the highest numbers of significant trends across all rainfall components are the northwestern Congo Basin and the broad western hinterlands that span the Tropical Wet and Tropical Dry regions. These two areas have changed significantly in almost all rainfall components, but this is not surprising because they correspond to the massive areas of statistically significant decreasing decadal trends across most rainfall components (Fig. 5). In contrast to the dominant areas of significant decreasing trend, the areas of increasing trend across all the rainfall components (the central Sahel, central-eastern Saharan region, the Niger Delta and coast of Liberia and Sierra Leone) are experiencing only mild changes overall, possibly because many of these increasing trends are not statistically significant.

Regionally, the Tropical Wet and Dry regions account for 59% of all significant trends across all rainfall components. The Equatorial (7%) and Saharan regions (12%) have the least number of significant trends across all rainfall components, while the Sahelian region accounts for 22% of all significant trends across all rainfall components (Table 4).

These analyses of the relative changes among the rainfall components support our hypothesis that disaggregated rainfall components are changing in different ways (with varying spatial distribution) in response to background warming because of differential sensitivity to climate dynamics (and possibly physiographic changes, e.g., deforestation). It also provides evidence that changes in rainfall totals are not necessarily the largest signals of rainfall change in West Africa.

3.6 – Relationship with ENSO

Since different rainfall components possess varying spatio-temporal trends, it is expected that each rainfall component will interact differently with ENSO, and this is explored here. The correlation analysis result to measure the association between ENSO and rainfall components in the study domain is shown in Fig. 9 below. The correlation coefficients are generally high, ranging on average from − 0.57 to + 0.57. The dominant spatial correlation pattern occurs in moderate rain-days, total rain-days, MDHR per year, and RSL. This pattern depicts a broad southwestward diagonal band of positive correlation coefficients, with clusters of significant grid-points in the coastal and the Sahelian regions. For the rainfall components mentioned above, negative correlation coefficients are found in the western Sahel, the Niger Delta, and the vast Tropical Wet region of the northwestern Congo Basin. In all, there is a considerable difference in the correlation between ENSO and these rainfall components for the western and eastern/central Sahel. Indeed, for all the rainfall components studied, the most consistent spatial correlation pattern is a dichotomy of ENSO teleconnection between the western Sahel and the eastern/central Sahel.

Further, the correlation coefficient pattern for annual rainfall totals is similar to that for annual rainfall intensity and heavy rain days. This pattern features a relatively strong positive correlation with ENSO in the eastern/central Sahel and weak positive to negative correlation coefficients in the western Sahel, with clusters of significant grid-points in both regions. Because the height of the WAM is in the boreal summer, the correlation between ENSO and JJAS rainfall was analyzed (Fig. 9a), and they show similar results to that in annual rainfall.

ENSO anomalies generally correlate well with global temperate changes, whereby El Niño leads to global positive temperature anomalies while La Nina leads to negative global temperature anomalies. However, ENSO correlation with rainfall is much more complex and non-linear. Increases in global precipitation with El Niño and decreases with La Nina have been observed (Adler et al., 2017) over local to regional scales, but ENSO signals over larger areas, such as the tropics or globally, are very weak (Wang et al., 2018; Gu & Adler, 2011; Su & Neelin, 2003). The correlation of ENSO with spatially averaged annual rainfall for the whole domain is very weak (-0.068 [not shown]) because of the combination of positive and negative correlations in the study domain. Even for all five regions, ENSO teleconnection is weak across all

rainfall components—except for rainfall onset and cessation in the Tropical Wet region (Fig. 9; Table 5). There are, however, sub-regional strong positive and negative ENSO correlations, especially in the central and western Sahel, parts of the Guinea Coast, and parts of the northwestern Congo Basin. The central Sahel has the most consistently strong and positive correlation with ENSO across all rainfall components, except rainfall onset and cessation. This result is corroborated by studies that have linked summer Sahelian rainfall (which is increasing in the central Sahel) to ENSO (Janicot et al., 1996; 2001).

Table 5
Association between ENSO and rainfall indices subdivided by region. Statistically significant trends ($p < 0.05$) are in bold, red font.

Rainfall components	Indices	Saharan	Tropical Wet	Tropical Dry	Sahelian	Equatorial
Rainfall Totals	Annual rainfall	0.072	-0.027	-0.033	0.004	-0.000
Rainfall Frequency	Total rain-days	0.148	-0.076	0.074	0.006	-0.101
Rainfall Intensity	Rainfall intensity	-0.002	0.003	-0.088	0.028	0.050
Rainfall Seasonality	Rainfall seasonality	0.017	0.036	-0.015	0.030	0.121
RSL	RSL	0.184	0.096	0.058	0.052	-0.072

The strength of central Sahelian teleconnection with ENSO is part of two domain-wide patterns of correlation: 1) for rainfall totals (annual and JJAS rainfall) and rainfall intensity—which have both been found to show a similar pattern of long-term trends, and 2) for rainfall frequency (moderate rainfall, total rain-days and MDHR per year). The similarity in the correlation patterns among the rainfall frequency indices is interesting because all three have the highest significant grid-points and are driving most of the changes happening in West Africa.

3.7 – ERA5 West Africa precipitation data validation

Supplementary Table S2 provides the correlation between monthly ground observation station rainfall data and monthly ERA5 data. In all stations, the correlation coefficient is very high, and in 95% of the stations, the Spearman rank correlation coefficient exceeds 0.8. Furthermore, the correlation of Mean precipitation and variability between ERA5 and the average for all stations are 0.95 and 0.75, respectively.

TAMSAT monthly rainfall contains significant missing data, nonetheless, monthly ERA5 precipitation is very high and positively correlated with monthly TRMM and TAMSAT rainfall across most of West Africa (Figs. 10 & 11). For both validation rainfall data, the correlation with ERA5 is more than 0.8 in more than 80% of the study area. The very sparse network of ground stations may explain the low to negative correlations in the Sahara Desert.

Iv. Summary And Conclusions

The overarching aim of this research is to examine the multi-decadal trends in various components of West African rainfall. Several studies have been conducted that held implications that rainfall totals alone may not carry the largest signal of rainfall changes from climate change, but most of these have not been explicitly detailed. Some prior research has either reported two oppositely trending rainfall components, or in the case of IPCC (2014), no significant trend in tropical rainfall totals – all of which imply that different rainfall components may vary considerably in terms of the magnitude of their contribution to the total signal of rainfall change in a region. Among other things, this study has sought to quantify these differences in the magnitude of change among the disaggregated rainfall components. Also, the sub-regional or spatial distribution of these signals of change have been examined, with the goal of not only providing information about the magnitude of change among the rainfall components, but also shedding light on the

locations of greatest (and least) change in each rainfall component, and then across all the rainfall components collectively. Individually and collectively, our analyses yielded the following results:

1. Rainfall frequency accounts for the greatest changes relative to all other rainfall components.

2. Rainfall totals and rainfall intensity are experiencing the second and third most changes, respectively.

3. Rainy season length (RSL) and rainfall seasonality, on the other hand, are seeing the least amount of change.

4. The Tropical Dry and Tropical Wet regions are experiencing the greatest changes in the entire study domain largely due to the changes in rainfall frequency and rainfall totals being concentrated in these two regions.

5. By contrast, the Saharan and Equatorial regions are the least-changing regions; changes in rainfall totals and rainfall frequency are minimal in these areas.

The signs of these changes are mostly negative and may be part of a broader trend of drying in tropical land areas and a consensus from previous research that anthropogenic changes drive these trends. Anthropogenic activities like land use/land cover changes are the main driver of the two most prominent local signals of change found in this study (that are mostly consistent with a growing number of studies):

1. The contrasting trends in rainfall totals and heavy rainfall between the central Sahel and the western Sahel.

2. The massive decreasing trend (in all rainfall components except light rainfall and rainfall onset) in the northwestern Congo Basin.

In all, West Africa remains one of the more vulnerable regions to climate change-induced rainfall. West Africa is still primarily a rain-fed agrarian economy and is thus more susceptible to the interannual fluctuations in rainfall frequency and rainfall totals. Drought and food insecurity in parts of the Sahel have led to civil and social unrest, like in the Horn of Africa. Yaro and Hesselberg (2016), drawing from IPCC's regional climate change report for West Africa and Africa (Niang et al., 2014; Reide et al., 2016), have detailed several mitigation and adaptation options available to West African governmental agencies and other stakeholders in combating the widespread drying and potential localized flooding in the region. But while policymakers should focus on rainfall frequency and rainfall totals, attention must be drawn to the practical role that other rainfall components such as rainfall timing and rainfall seasonality play in the livelihood of West African people. It has been shown that the timing of the rainy season is more important for a productive growing season than rainfall amount. A year with normal (or above normal) rainfall totals but marked by delayed onset and/or premature cessation of the rainy season is worse for plants than one with a substantial shortfall in total amount but with normal dates of onset and cessation.

The results of this study challenge the widespread acceptance of rainfall totals as the only representation of rainfall, especially on regional to large scales. Components of rainfall frequency, such as rain-days, which show daily occurrences rather than accumulated amount, are perhaps more robust representations of the regional rainfall climatology than rainfall totals. Rainfall frequency appears to accurately depict the migration of the tropical rain belt, compared to rainfall totals that show local variations in rainfall due to elevation (Fig. 3). Rainfall frequency likely captures MCSs or large-scale rainfall-producing systems better, which may have important implications for future rainfall predictions in the domain. CMIP5 estimates of future rainfall changes in West Africa have a low to medium confidence, with considerable inter-model variation (Niang et al., 2014), partially attributable to the well-known inability of GCMs to resolve convective rainfall. The use of rainfall frequency in place of rainfall totals should be explored in future research to see how well it improves future estimates of rainfall changes in the West African region. Additionally, it would be interesting to explore the relative magnitude and direction of rainfall component changes in the broader

tropics and temperate climates where precipitation plays a less prominent role. Interdependencies among the rainfall components can also be assessed at various spatial scales.

Declarations

ACKNOWLEDGEMENT

This research was improved considerably by the suggestions of Dr. Scott Sheridan and Dr. Thomas Schmidlin in the Department of Geography at Kent State University. The authors are also grateful to Eric Tyler Smith and Ryan Adams for their help with MATLAB coding.

Funding

The authors did not receive support from any organization for the submitted work

Conflict of Interest/Competing interests/Financial interests

The authors have no conflict of interest. The authors have no relevant financial or non-financial interests to disclose.

Availability of data and material

Precipitation data used in this study is publicly available at their respective website and data repository as cited in this study.

Code Availability

MATLAB software was used entirely. Codes are available from the corresponding author on reasonable request.

Author's Contribution

All authors contributed to the study conception and design. Material preparation, data collection and analysis were performed by [Omon Obarein] and [Cameron Lee]. The first draft of the manuscript was written by [Omon Obarein] and all authors commented on previous versions of the manuscript. All authors read and approved the final manuscript.

Ethics approval

The authors have looked over the ethical guidelines of the journal and we assure that we have complied with all ethical standards.

Consent to participate

NA

Consent for publication

All authors gave their full consent to submit this work, and this submission does not violate any rules of Kent State University

References

1. Adefolalu DO (1986) Further aspects of Sahelian drought as evident from rainfall regime of Nigeria. *Archives for meteorology, geophysics, and bioclimatology, Series B*, **36**(3–4): 277–295
2. Adler RF, Gu G, Sapiano M, Wang JJ, Huffman GJ (2017) Global precipitation: Means, variations and trends during the satellite era (1979–2014). Surv Geophys 38(4):679–699
3. Akinsanola AA, Zhou W (2019) Dynamic and thermodynamic factors controlling increasing summer monsoon rainfall over the West African Sahel. Clim Dyn 52(7–8):4501–4514
4. Akumaga U, Tarhule A (2018) Projected Changes in Intra-Season Rainfall Characteristics in the Niger River Basin, West Africa. Atmosphere 9(12):497
5. Alpert P, Ben-Gai T, Baharad A, Benjamini Y, Yekutieli D, Colacino M, … and Michaelides S (2002) The paradoxical increase of Mediterranean extreme daily rainfall in spite of decrease in total values. Geophysical research letters 29(11):31–31
6. Anyamba A, Tucker CJ (2005) Analysis of Sahelian vegetation dynamics using NOAA-AVHRR NDVI data from 1981–2003. Journal of arid environments 63(3):596–614
7. Aryeetey-Attoh S, McDade BE (1997) Geography of Sub-Saharan Africa. Prentice Hall, Upper Saddle River
8. Asefi-Najafabady S, Saatchi S (2013) Response of African humid tropical forests to recent rainfall anomalies. Philosophical Transactions of the Royal Society B: Biological Sciences 368(1625):20120306
9. Ayoade JO (2004) Introduction to climatology for the Tropics Ibadan. *Spectrum Book*
10. Balas N, Nicholson SE, Klotter D (2007) The relationship of rainfall variability in West Central Africa to sea-surface temperature fluctuations. International Journal of Climatology: A Journal of the Royal Meteorological Society 27(10):1335–1349
11. Biasutti M (2013) Forced Sahel rainfall trends in the CMIP5 archive. Journal of Geophysical Research: Atmospheres 118(4):1613–1623
12. Bichet A, Diedhiou A (2018) West African Sahel has become wetter during the last 30 years, but dry spells are shorter and more frequent. Climate Res 75(2):155–162
13. Camargo SJ, Sobel AH (2005) Western North Pacific tropical cyclone intensity and ENSO. J Clim 18(15):2996–3006
14. Camberlin P, Moron V, Okoola R, Philippon N, Gitau W (2009) Components of rainy seasons' variability in Equatorial East Africa: onset, cessation, rainfall frequency and intensity. Theoretical applied climatology 98(3–4):237–249
15. Camberlin P, Kpanou M, Roucou P (2020) Classification of Intense Rainfall Days in Southern West Africa and Associated Atmospheric Circulation. Atmosphere 11(2):188
16. Carvalho MJ, Melo-Gonçalves P, Teixeira JC, Rocha A (2016) Regionalization of Europe based on a K-Means Cluster Analysis of the climate change of temperatures and precipitation. Physics Chemistry of the Earth Parts A/B/C 94:22–28
17. Chadwick R, Boutle I, Martin G (2013) Spatial patterns of precipitation change in CMIP5: Why the rich do not get richer in the tropics. J Clim 26(11):3803–3822
18. Choudhury SK, Sa PK, Choo KKR, Bakshi S (2017) Segmenting foreground objects in a multi-modal background using modified Z-score. *Journal of Ambient Intelligence and Humanized Computing*, 1–15

19. Crétat J, Vizy EK, Cook KH (2015) The relationship between African easterly waves and daily rainfall over West Africa: observations and regional climate simulations. Clim Dyn 44(1–2):385–404
20. Dahlman L (2016) Climate variability: Oceanic Nino Index. https://www.climate.gov/news-features/understanding-climate/climate-variability-oceanic-niño-index (accessed 14 August 2020)
21. Dee D, Fasullo J, Shea D, Walsh J & National Center for Atmospheric Research Staff (Eds). 2016. "The Climate Data Guide: Atmospheric Reanalysis: Overview & Comparison Tables." https://climatedataguide.ucar.edu/climate-data/atmospheric-reanalysis-overview-comparison-tables (accessed 14 August 2020)
22. Dee, Dick & National Center for Atmospheric Research Staff (Eds). Last modified 03 Jul 2021. "The Climate Data Guide: ERA5 atmospheric reanalysis." Retrieved from https://climatedataguide.ucar.edu/climate-data/era5-atmospheric-reanalysis
23. Delhasse A, Kittel C, Amory C, Hofer S, Fettweis X (2019) Brief communication: Interest of a regional climate model against ERA5 to simulate the near-surface climate of the Greenland ice sheet. *The Cryosphere Discussions*
24. Diallo I, Giorgi F, Deme A, Tall M, Mariotti L, Gaye AT (2016) Projected changes of summer monsoon extremes and hydroclimatic regimes over West Africa for the twenty-first century. Climate dynamics 47(12):3931–3954
25. Dong B, Sutton R (2015) Dominant role of greenhouse-gas forcing in the recovery of Sahel rainfall. Nature Climate Change 5(8):757
26. Dore MH (2005) Climate change and changes in global precipitation patterns: what do we know? Environment international 31(8):1167–1181
27. Dunning CM, Black E, Allan RP (2018) Later wet seasons with more intense rainfall over Africa under future climate change. J Clim 31(23):9719–9738
28. EarthDATA GIOVANNI (2021) TRMM data. Retrieved from https://giovanni.gsfc.nasa.gov/giovanni/
29. Erfanian A, Wang G, Yu M, Anyah R (2016) Multimodel ensemble simulations of present and future climates over West Africa: Impacts of vegetation dynamics. Journal of advances in modeling Earth systems 8(3):1411–1431
30. Feng X, Porporato A, Rodriguez-Iturbe I (2013) Changes in rainfall seasonality in the tropics. Nature Climate Change 3(9):811
31. Feng H, Zhang M (2015) Global land moisture trends: drier in dry and wetter in wet over land. Scientific reports 5(1):1–6
32. Gaetani M, Flamant C, Bastin S, Janicot S, Lavaysse C, Hourdin F, … Bony S (2017) West African monsoon dynamics and precipitation: the competition between global SST warming and CO 2 increase in CMIP5 idealized simulations. Climate dynamics 48(3–4):1353–1373
33. Ghoneim E, El-Baz F (2020) Satellite Image Data Integration for Groundwater Exploration in Egypt. In: Environmental Remote Sensing in Egypt. Springer, Cham, pp 211–230
34. Giannini A, Salack S, Lodoun T, Ali A, Gaye AT, Ndiaye O (2013) A unifying view of climate change in the Sahel linking intra-seasonal, interannual and longer time scales. Environmental Research Letters 8(2):024010
35. Gleixner S, Demissie T, Diro GT (2020) Did ERA5 Improve Temperature and Precipitation Reanalysis over East Africa? Atmosphere 11(9):996
36. *GPCC Precipitation data provided by the NOAA/OAR/ESRL PSL, Boulder, Colorado, USA, from their Web site a t*GPCC Precipitation Data Set: NOAA Physical Sciences Laboratory
37. Greve P, Orlowsky B, Mueller B, Sheffield J, Reichstein M, Seneviratne SI (2014) Global assessment of trends in wetting and drying over land. Nat Geosci 7(10):716–721
38. Gu G, Adler RF (2011) Precipitation and temperature variations on the interannual time scale: Assessing the impact of ENSO and volcanic eruptions. J Clim 24(9):2258–2270

39. Harris I, Jones PD, Osborn TJ, Lister DH (2014) CRU TS3. 22: Climatic Research Unit (CRU) Time-Series (TS) Version 3.22 of High Resolution Gridded Data of Month-by-month Variation in Climate (Jan. 1901-Dec. 2013). *NCAS British Atmospheric Data Centre, 24th September, 2016*
40. Hagos SM, Cook KH (2007) Dynamics of the West African monsoon jump. J Clim 20(21):5264–5284
41. Hannachi A (2004) A primer for EOF analysis of climate data. *Department of Meteorology, University of Reading*, 1–33
42. He J, Johnson NC, Vecchi GA, Kirtman B, Wittenberg AT, Sturm S (2018) Precipitation sensitivity to local variations in tropical sea surface temperature. J Clim 31(22):9225–9238
43. Hoffmann L, Günther G, Li D, Stein O, Wu X, Griessbach S, …Wright JS (2019) From ERA-Interim to ERA5: the considerable impact of ECMWF's next-generation reanalysis on Lagrangian transport simulations. Atmos Chem Phys 19(5):3097–3124
44. Hu Z, Chen X, Chen D, Li J, Wang S, Zhou Q, …Guo M (2019) "Dry gets drier, wet gets wetter": A case study over the arid regions of central Asia. Int J Climatol 39(2):1072–1091
45. Hua W, Zhou L, Chen H, Nicholson SE, Raghavendra A, Jiang Y (2016) Possible causes of the Central Equatorial African long-term drought. Environmental Research Letters 11(12):124002
46. IPCC (2021) Climate Change 2021: The Physical Science Basis. Contribution of Working Group I to the Sixth Assessment Report of the Intergovernmental Panel on Climate Change [Masson-Delmotte, V., P. Zhai, A. Pirani, S. L. Connors, C. Péan, S. Berger, N. Caud, Y. Chen, L. Goldfarb, M. I. Gomis, M. Huang, K. Leitzell, E. Lonnoy, J. B. R. Matthews, T. K. Maycock, T. Waterfield, O. Yelekçi, R. Yu and B. Zhou (eds.)]. Cambridge University Press. In Press
47. Janicot S, Moron V, Fontaine B (1996) Sahel droughts and ENSO dynamics. Geophys Res Lett 23(5):515–518
48. Janicot S, Trzaska S, Poccard I (2001) Summer Sahel-ENSO teleconnection and decadal time scale SST variations. Clim Dyn 18(3–4):303–320
49. Jiang Y, Zhou L, Tucker CJ, Raghavendra A, Hua W, Liu YY, Joiner J (2019) Widespread increase of boreal summer dry season length over the Congo rainforest. Nature Climate Change 9(8):617–622
50. Jin D, Huo L (2018) Influence of tropical Atlantic sea surface temperature anomalies on the East Asian summer monsoon. Q J R Meteorol Soc 144(714):1490–1500
51. Kanemasu ET, Stewart JI, van Donk SJ, Virmani SM (1990) Agroclimatic approaches for improving agricultural productivity in semi-arid tropics. Adv Soil Sci 13:273–309
52. Kelley OA (2014) Where the least rainfall occurs in the Sahara Desert, the TRMM radar reveals a different pattern of rainfall each season. J Clim 27(18):6919–6939
53. Kwak SK, Kim JH (2017) Statistical data preparation: management of missing values and outliers. Korean journal of anesthesiology 70(4):407
54. LeCompte D, Tinker R, Dionne J, Halpert M, Thiao W (1994) Wettest rainy season in 30 years across African Sahel. Special Climate Summary 94(2):5
55. Lee CC (2020) Trends and variability in air mass frequencies: indicators of a changing climate. Journal of Climate (Accepted, in press), DOI: 10.1175/JCLI-D-20-0094.1
56. Lee JH, Yang CY, Julien PY (2020) Taiwanese rainfall variability associated with large-scale climate phenomena. Adv Water Resour 135:103462
57. Leys C, Ley C, Klein O, Bernard P, Licata L (2013) Detecting outliers: Do not use standard deviation around the mean, use absolute deviation around the median. J Exp Soc Psychol 49(4):764–766
58. Lodoun T, Giannini A, Traore PS, Some L, Sanon M, Vaksmann M, Rasolodimby JM (2013) Changes in seasonal descriptors of precipitation in Burkina Faso associated with late 20th century drought and recovery in West Africa.

Environmental Development 5:96–108

59. Mahe GIL, L'hote Y, Olivry JC, Wotling G (2001) Trends and discontinuities in regional rainfall of West and Central Africa: 1951–1989. Hydrol Sci J 46(2):211–226
60. Mahto SS, Mishra V (2019) Does ERA-5 outperform other reanalysis products for hydrologic applications in India? Journal of Geophysical Research: Atmospheres 124(16):9423–9441
61. Maidment RI, Grimes D, Black E, Tarnavsky E, Young M, Greatrex H, … Alcántara EMU (2017) A new, long-term daily satellite-based rainfall dataset for operational monitoring in Africa. Scientific data 4(1):1–19
62. Maidment RI, Grimes D, Allan RP, Tarnavsky E, Stringer M, Hewison T, … Black E (2014) The 30 year TAMSAT African rainfall climatology and time series (TARCAT) data set. Journal of Geophysical Research: Atmospheres 119(18):10–619
63. Malhi Y, Wright J (2004) Spatial patterns and recent trends in the climate of tropical rainforest regions. Philosophical Transactions of the Royal Society of London Series B: Biological Sciences 359(1443):311–329
64. Manatsa D, Mushore T, Lenouo A (2017) Improved predictability of droughts over southern Africa using the standardized precipitation evapotranspiration index and ENSO. Theoretical applied climatology 127(1–2):259–274
65. Mohino E, Janicot S, Bader J (2011) Sahel rainfall and decadal to multi-decadal sea surface temperature variability. Climate dynamics 37(3–4):419–440
66. Monerie PA, Sanchez-Gomez E, Gaetani M, Mohino E, Dong B (2020) Future evolution of the Sahel precipitation zonal contrast in CESM1. Climate dynamics 55(9):2801–2821
67. Monerie PA, Wainwright CM, Sidibe M, Akinsanola AA (2020) Model uncertainties in climate change impacts on Sahel precipitation in ensembles of CMIP5 and CMIP6 simulations. Clim Dyn 55(5):1385–1401
68. Monerie PA, Sanchez-Gomez E, Pohl B, Robson J, Dong B (2017) Impact of internal variability on projections of Sahel precipitation change. Environmental Research Letters 12(11):114003
69. Moron V, Robertson AW, Ward MN (2006) Seasonal predictability and spatial coherence of rainfall characteristics in the tropical setting of Senegal. Mon Weather Rev 134(11):3248–3262
70. Mubvuma MT (2013) Climate change: matching growing season length with maize crop varietal life cycles in semi-arid regions of Zimbabwe. Greener jour of agricultural sciences 3(12):809–816
71. Mugalavai EM, Kipkorir EC, Raes D, Rao MS (2008) Analysis of rainfall onset, cessation and length of the growing season for western Kenya. Agriculture Forest Meteorology 148:1123–1135
72. Neelin JD, Münnich M, Su H, Meyerson JE, Holloway CE (2006) Tropical drying trends in global warming models and observations. *Proceedings of the National Academy of Sciences*, **103**(16): 6110–6115
73. Niang I, Ruppel OC, Abdrabo MA, Essel A, Lennard C, Padgham J, Urquhart P (2014) Africa. In: Climate Change 2014: Impacts, Adaptation, and Vulnerability. Part B: Regional Aspects. Contribution of Working Group II to the Fifth Assessment Report of the Intergovernmental Panel on Climate Change [Barros, V.R., C.B. Field, D.J. Dokken, M.D. Mastrandrea, K.J. Mach, T.E. Bilir, M. Chatterjee, K.L. Ebi, Y.O. Estrada, R.C. Genova, B. Girma, E.S. Kissel, A.N. Levy, S. MacCracken, P .R. Mastrandrea, and L.L. White (eds.)]. Cambridge University Press, Cambridge, United Kingdom and New York, NY, USA, pp. 1199–1265
74. Nicholson SE (1979) Revised rainfall series for the West African subtropics. Mon Weather Rev 107(5):620–623
75. Nicholson SE (1980) The nature of rainfall fluctuations in subtropical West Africa. Mon Weather Rev 108(4):473–487
76. Nicholson SE (1993) An overview of African rainfall fluctuations of the last decade. J Clim 6(7):1463–1466
77. Nicholson SE, Ba MB, Kim JY (1996) Rainfall in the Sahel during 1994. J Clim 9(7):1673–1676

78. Nicholson SE (2009) A revised picture of the structure of the "monsoon" and land ITCZ over West Africa. Clim Dyn 32(7–8):1155–1171
79. Nicholson SE, Funk C, Fink AH (2018) Rainfall over the African continent from the 19th through the 21st century. Glob Planet Change 165:114–127
80. Nkrumah F, Vischel T, Panthou G, Klutse NAB, Adukpo DC, Diedhiou A (2019) Recent Trends in the Daily Rainfall Regime in Southern West Africa. Atmosphere 10(12):741
81. Nogherotto R, Coppola E, Giorgi F, Mariotti L (2013) Impact of Congo Basin deforestation on the African monsoon. Atmospheric Science Letters 14(1):45–51
82. Obarein OA, Amanambu AC (2019) Rainfall timing: variation, characteristics, coherence, and interrelationships in Nigeria. Theoret Appl Climatol 137(3–4):2607–2621
83. Ohlson JA, Kim S (2015) Linear valuation without OLS: the Theil-Sen estimation approach. Rev Acc Stud 20(1):395–435
84. Olaniran OJ (2002) Rainfall anomalies in Nigeria: The contemporary understanding. An inaugural lecture of the Department of Geography, University of Ilorin, Ilorin. Nigeria
85. Olauson J (2018) ERA5: The new champion of wind power modelling? Renewable energy 126:322–331
86. Owusu K, Waylen P (2009) Trends in spatio-temporal variability in annual rainfall in Ghana (1951-2000). Weather 64(5):115–120
87. Riede JO, Posada R, Fink AH, Kaspar F (2016) What's on the 5th IPCC Report for West Africa? In: Adaptation to Climate Change and Variability in Rural West Africa. Springer, Cham, pp 7–23
88. Sanogo S, Fink AH, Omotosho JA, Ba A, Redl R, Ermert V (2015) Spatio-temporal characteristics of the recent rainfall recovery in West Africa. Int J Climatol 35(15):4589–4605
89. Schneider U, Becker A, Finger P, Meyer-Christoffer A, Ziese M, Rudolf B (2014) GPCC's new land surface precipitation climatology based on quality-controlled in situ data and its role in quantifying the global water cycle. Theoret Appl Climatol 115(1):15–40
90. Sen PK (1968) Estimates of the regression coefficient based on Kendall's tau. Journal of the American statistical association 63(324):1379–1389
91. Singh K, Xie M (2008) Bootstrap: a statistical method. *Unpublished manuscript, Rutgers University, USA.* http://www.stat. rutgers. edu/home/mxie/RCPapers/bootstrap. Pdf (accessed 14 August 2020)
92. Srivastava AK, Kothawale DR, Rajeevan MN (2017) Variability and long-term changes in surface air temperatures over the Indian subcontinent. In: Observed climate variability and change over the Indian region. Springer, Singapore, pp 17–35
93. Stocker TF, Clarke GKC, Le Treut H, Lindzen RS, Meleshko VP, Mugara RK, … Holtslag AAM (2001) Physical climate processes and feedbacks. In: IPCC, 2001: Climate Change 2001: The Scientific Basis. Contribution of Working Group I to the Third Assessment Report of the Intergovernmental Panel on Climate Change. Cambridge University Press, pp 417–470
94. Su H, Neelin JD (2003) The scatter in tropical average precipitation anomalies. J Clim 16(23):3966–3977
95. Sylla MB, Nikiema PM, Gibba P, Kebe I, Klutse NAB (2016) Climate change over West Africa: Recent trends and future projections. In: Adaptation to climate change and variability in rural West Africa. Springer, Cham, pp 25–40
96. Tarnavsky E, Grimes D, Maidment R, Black E, Allan RP, Stringer M, … Kayitakire F (2014) Extension of the TAMSAT satellite-based rainfall monitoring over Africa and from 1983 to present. Journal of Applied Meteorology Climatology 53(12):2805–2822

97. Theil H (1950) A rank-invariant method of linear and polynomial regression analysis. Indagationes mathematicae 12(85):173
98. Trenberth KE et al in IPCC Climate Change 2007: The Physical Science Basis (eds Solomon, S. et al.) Ch. 3 (Cambridge Univ. Press, 2007), Feng X, Porporato A, & Rodriguez-Iturbe, I. (2013)
99. Trewin B (2014) The climates of the Tropics and how they are changing. *State Trop*, 39–51
100. Urraca R, Huld T, Gracia-Amillo A, Martinez-de-Pison FJ, Kaspar F, Sanz-Garcia A (2018) Evaluation of global horizontal irradiance estimates from ERA5 and COSMO-REA6 reanalyses using ground and satellite-based data. Sol Energy 164:339–354
101. Wang B, Li J, Cane MA, Liu J, Webster PJ, Xiang B, … Ha KJ (2018) Toward predicting changes in the land monsoon rainfall a decade in advance. J Clim 31(7):2699–2714
102. Wang G, Ahmed KF, You L, Yu M, Pal J, Ji Z (2017) Projecting regional climate and cropland changes using a linked biogeophysical-socioeconomic modeling framework: 1. Model description and an equilibrium application over West Africa. J Adv Model Earth Syst 9(1):354–376
103. Wang M, Guo JR, Song J, Fu YZ, Sui WY, Li YQ, … Zuo WT (2020) The correlation between ENSO events and sea surface temperature anomaly in the Bohai Sea and Yellow Sea. *Regional Studies in Marine Science*, 101228
104. Wilks D (2016) "The stippling shows statistically significant grid points": How research results are routinely overstated and overinterpreted, and what to do about it. Bull Am Meteor Soc 97(12):2263–2273
105. Xu ZX, Takeuchi K, Ishidaira H (2004) Correlation between El Niño–Southern Oscillation (ENSO) and precipitation in South-east Asia and the Pacific region. Hydrological processes 18(1):107–123
106. Yaro JA, Hesselberg J (eds) (2016) Adaptation to climate change and variability in rural West Africa. Springer International Publishing
107. Zhang X, Zwiers FW, Hegerl GC, Lambert FH, Gillett NP, SolomonS, … Nozawa T (2007) Detection of human influence on twentieth-century precipitation trends. Nature 448(7152):461–465
108. Zhang Y, Cai C, Chen B, Dai W (2019) Consistency evaluation of precipitable water vapor derived from ERA5, ERA-Interim, GNSS, and radiosondes over China. Radio Science 54(7):561–571
109. Zhou L, Tian Y, Myneni RB, Ciais P, Saatchi S, Liu YY, … Hwang T (2014) Widespread decline of Congo rainforest greenness in the past decade. Nature 509(7498):86–90

Figures

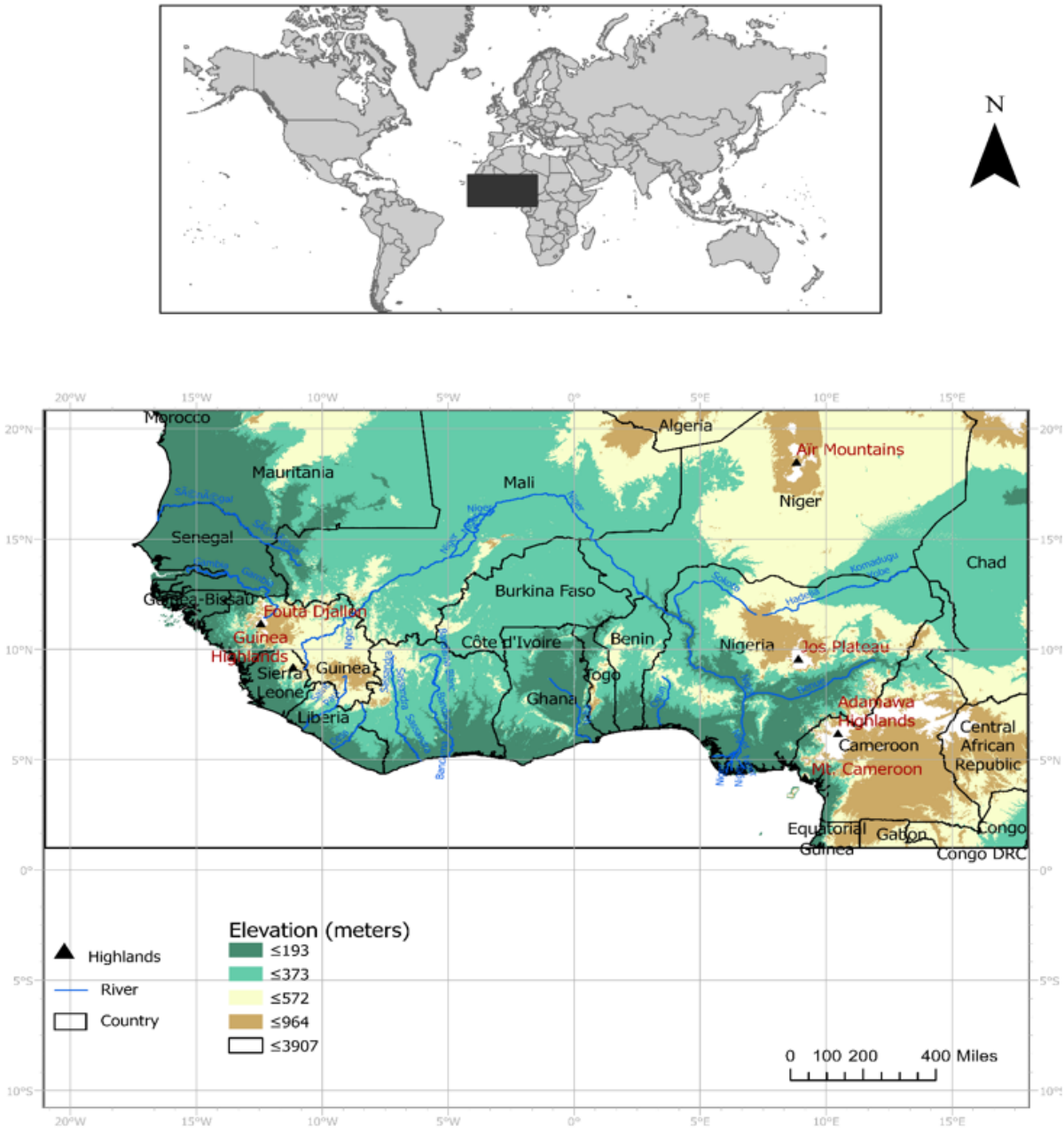

Figure 1

Relief and drainage map of West Arica. Inset map showing West African domain

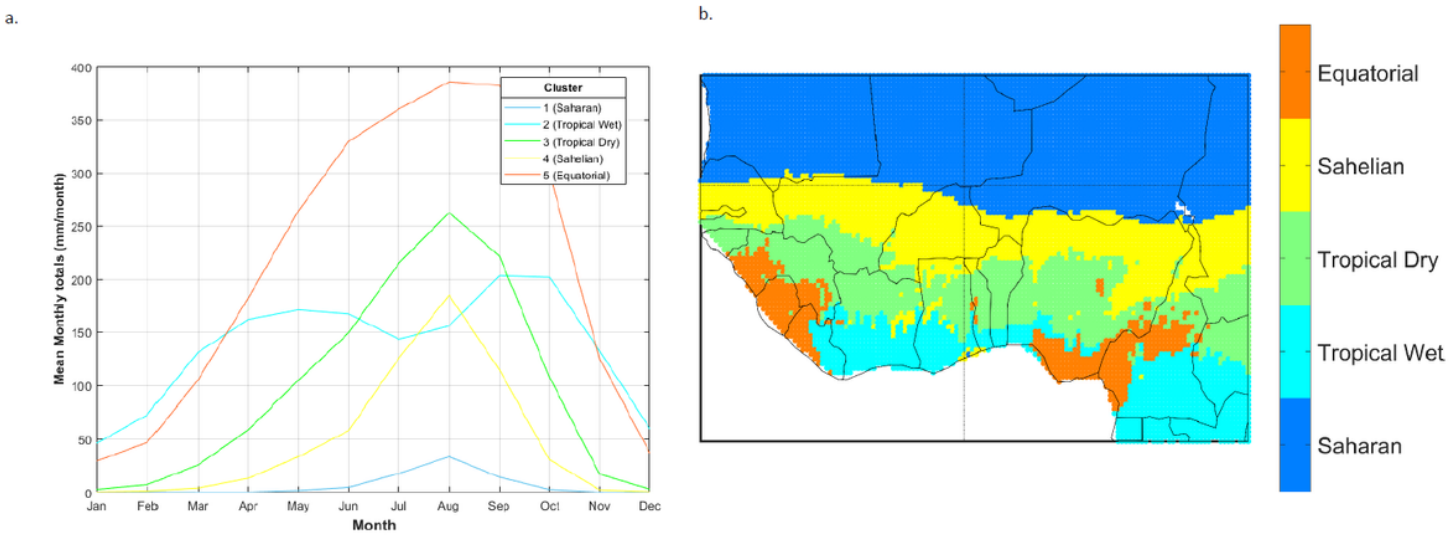

Figure 2

(a) Mean annual cycle of rainfall totals for the five cluster regions (b) Regionalized clusters of monthly rainfall totals (1979 – 2018).

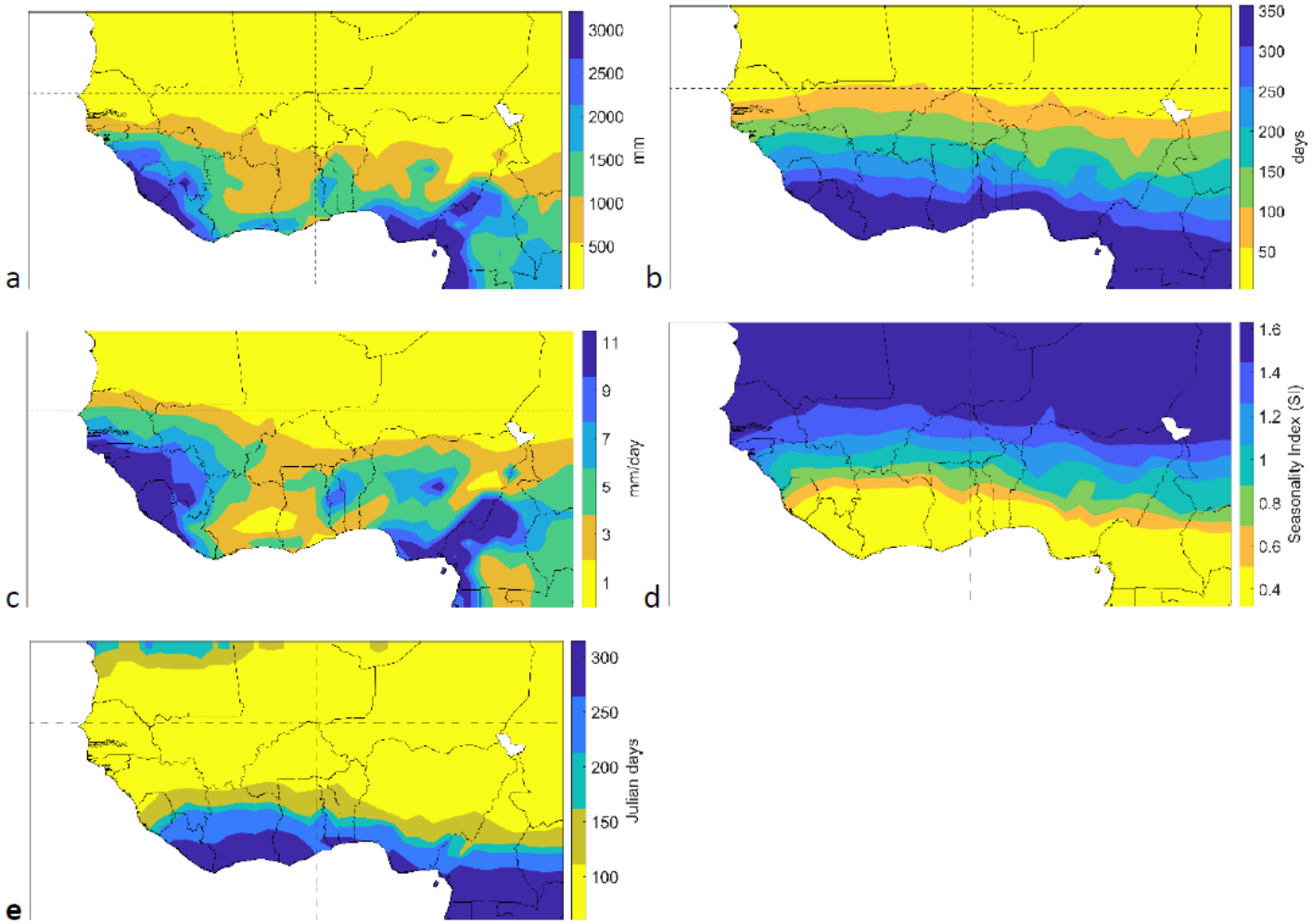

Figure 3

Long-term means of (a) annual rainfall, (b) annual number of rain days, (c) annual rainfall intensity, (d) seasonality, (e) RSL (1979 – 2018). Note the different scale for each plot

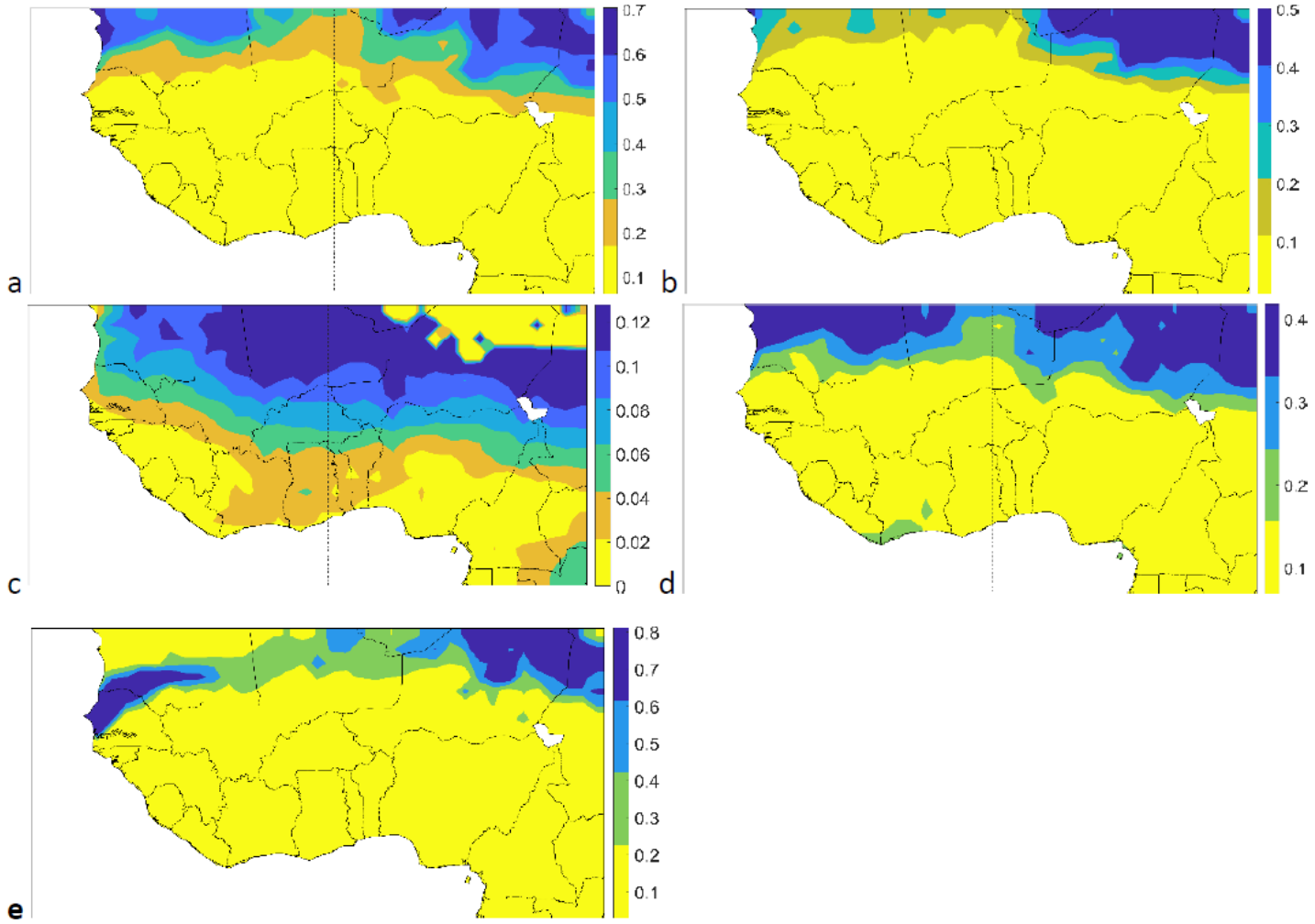

Figure 4

Spatially relative/Normalized Interannual variability in (a) annual rainfall, (b) annual number of rain days, (c) annual rainfall intensity, (d) seasonality, (e) RSL (1979 – 2018). Note the different scale and absence of unit for each plot

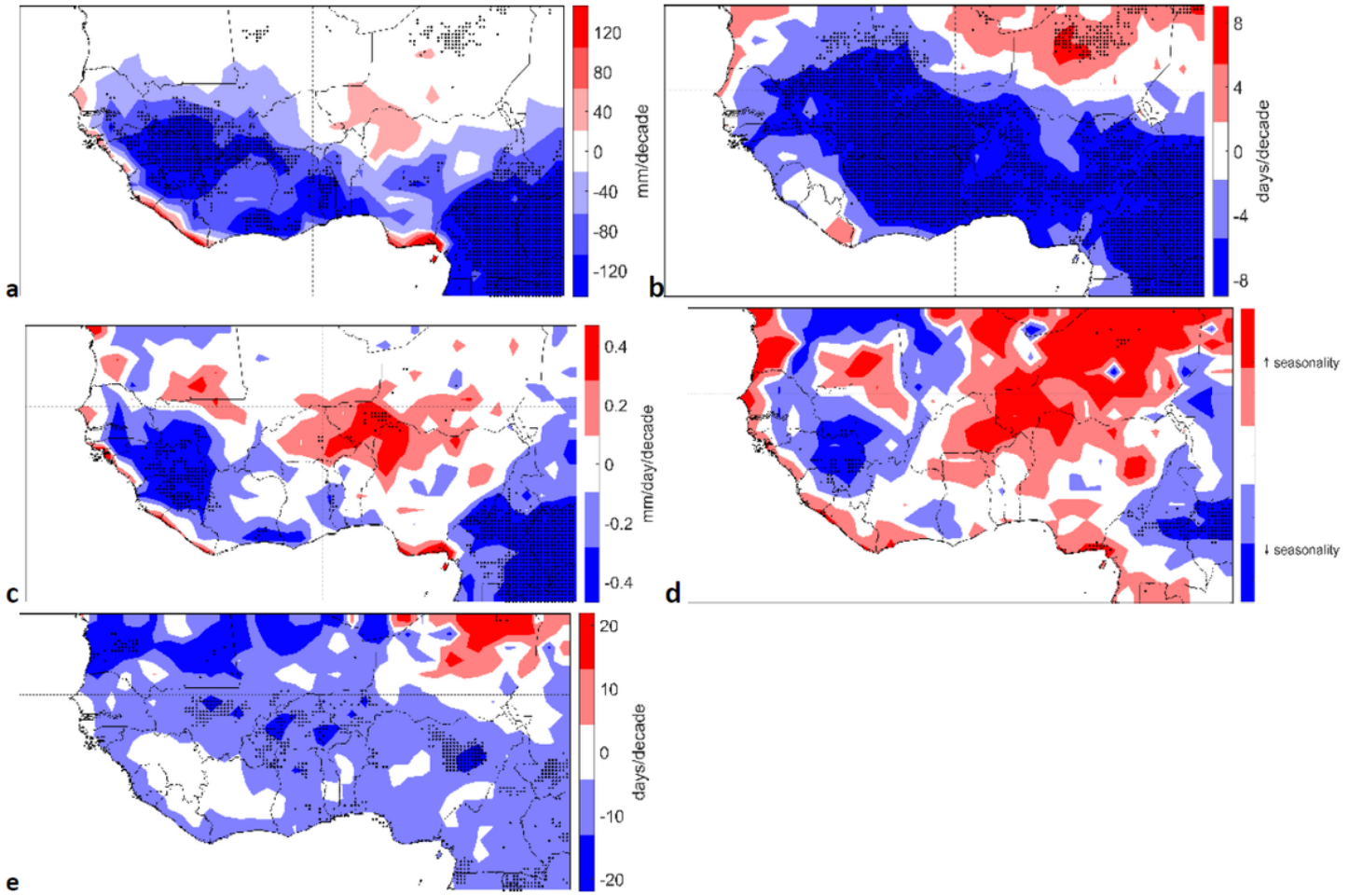

Figure 5

Decadal changes in (a) annual rainfall, (b) annual number of rain-days, (c) annual rainfall intensity, (d) seasonality, (e) RSL (1979 – 2018). Black stippling represents significant ($p<0.05$) grid-point trends. Note the different scale for each plot.

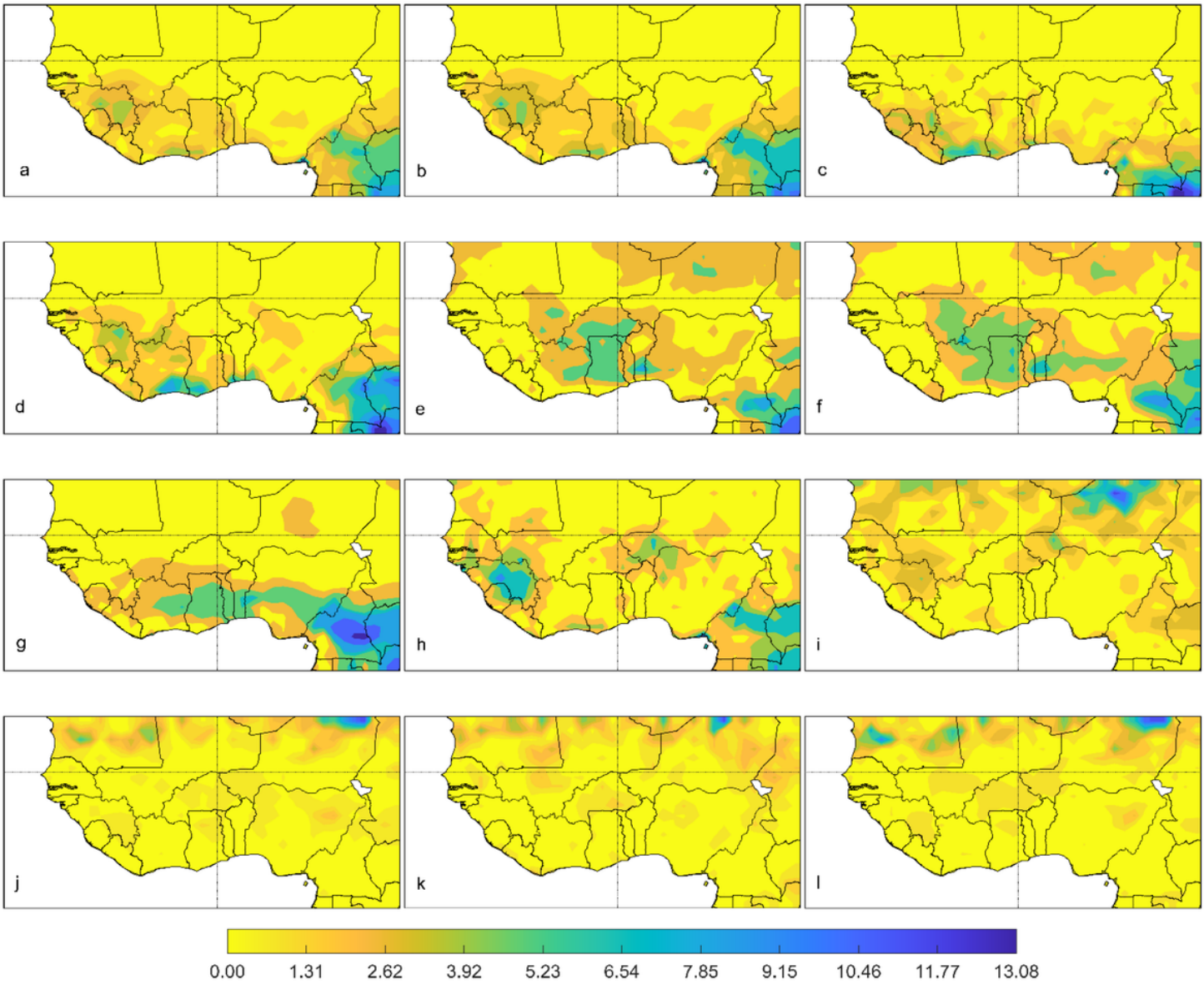

Figure 6

Absolute z-scores of the trends in (a) daily rainfall (b) annual rainfall (c) Light rainfall (d) Heavy rainfall (e) Moderate rainfall (f) annual number of rain-days, (g) MDHR per year, (h) annual rainfall intensity, (i) mean seasonality, (j) rainfall onset dates, (k) rainfall cessation dates, (l) RSL. 1979 – 2018.

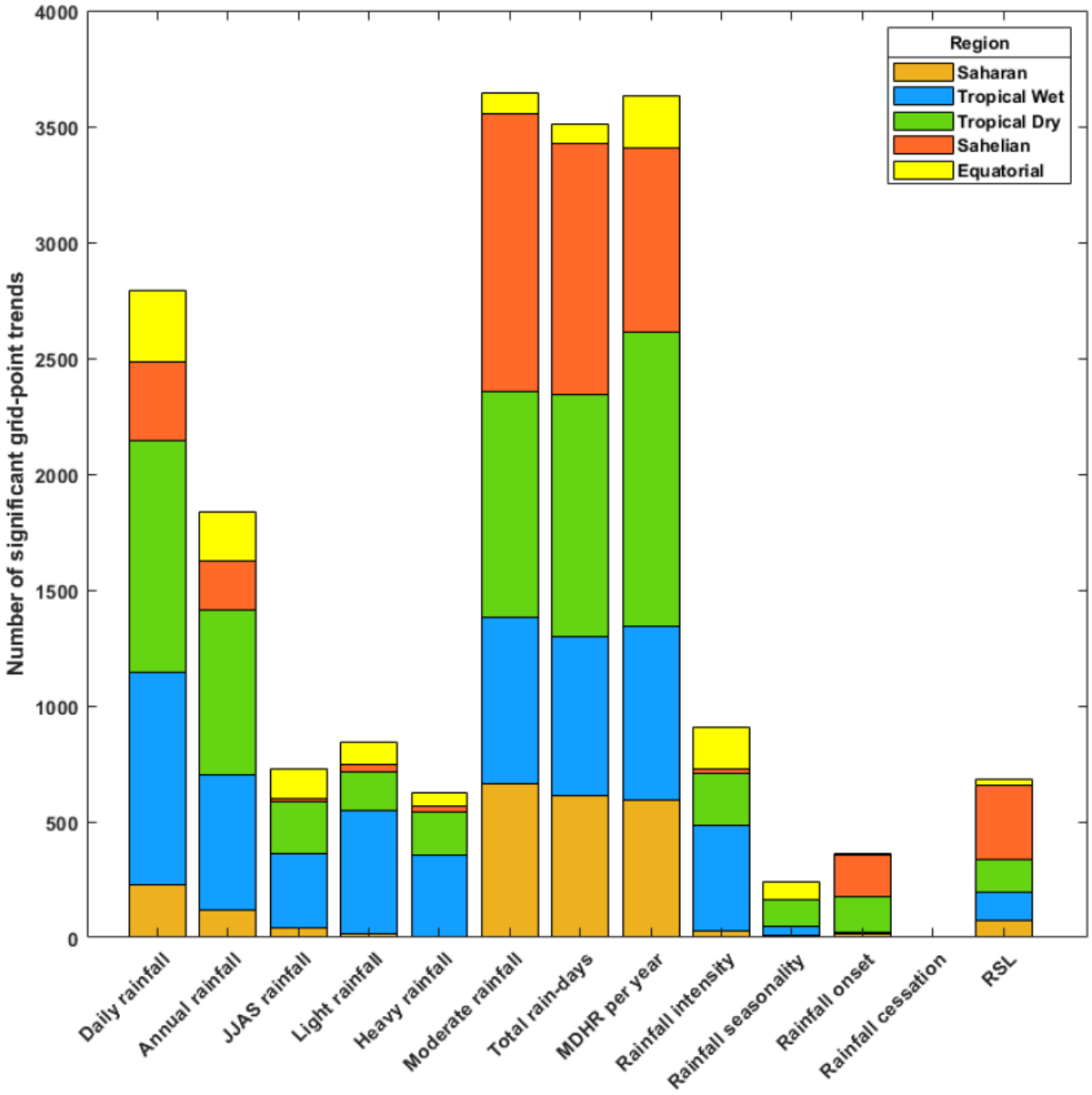

Figure 7

Sum of total significant grid-points in each region, by rainfall indices.

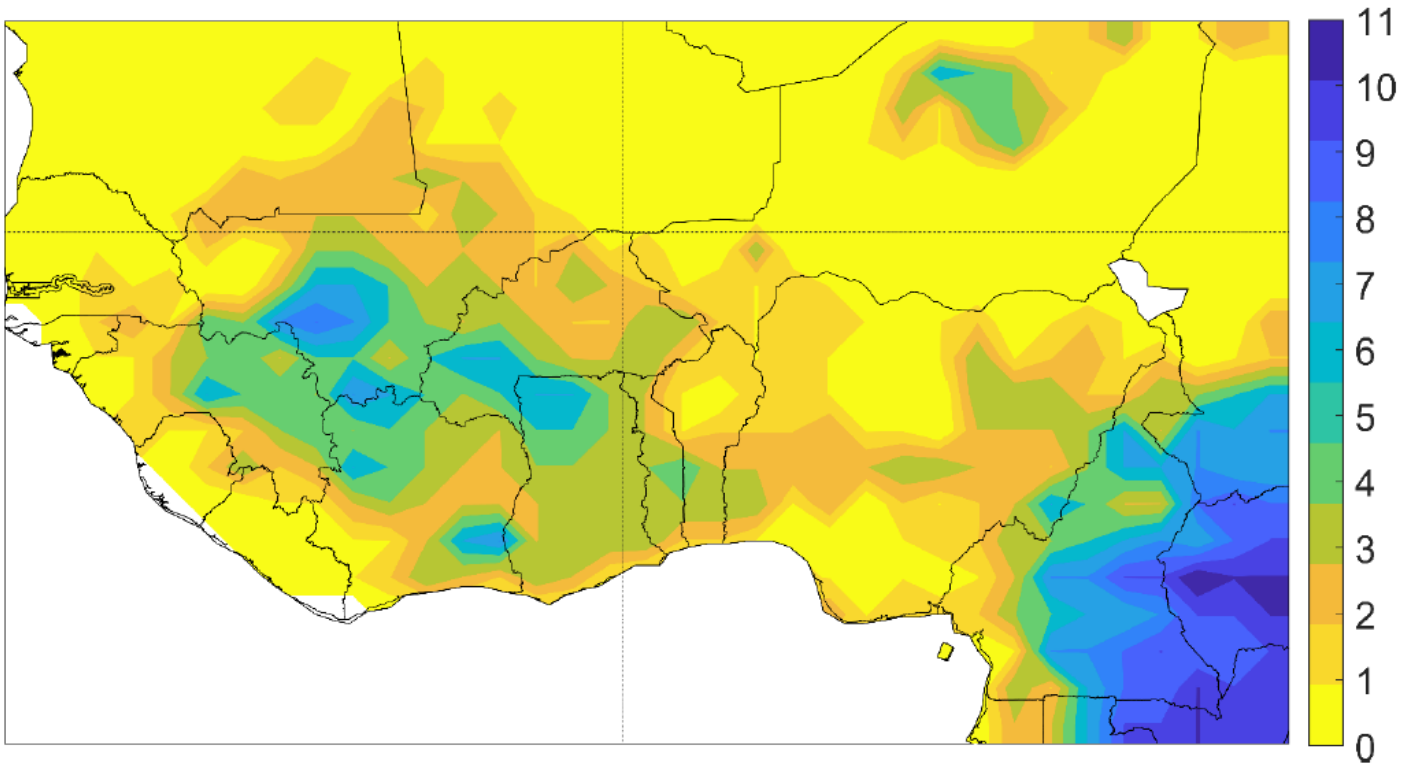

Figure 8

Total number of statistically significant trends across all rainfall indices for each grid-point

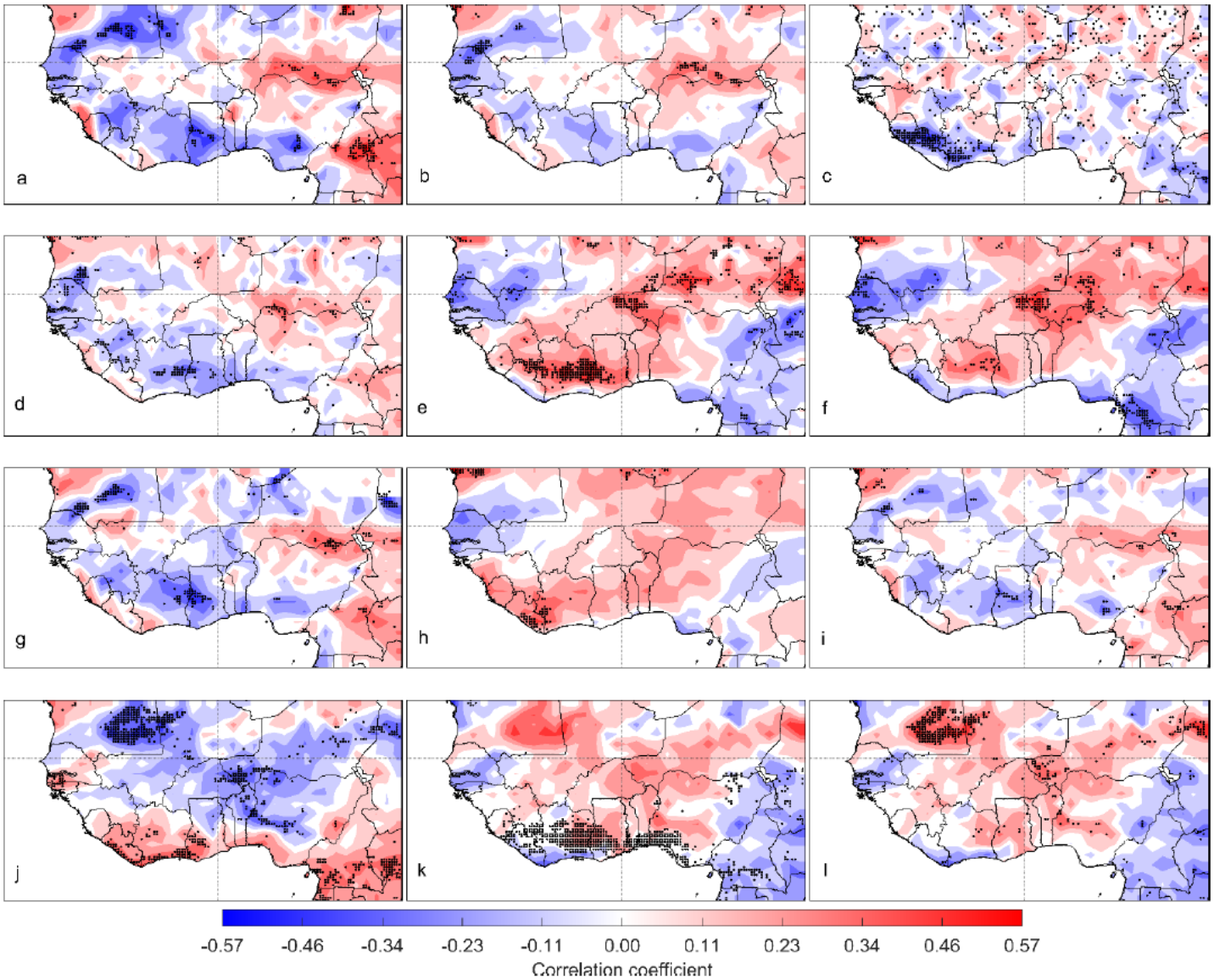

Figure 9

Association between ENSO and (a) JJAS rainfall (b) annual rainfall (c) Light rainfall (d) Heavy rainfall (e) Moderate rainfall (f) annual number of rain-days (g) annual rainfall intensity (h) MDHR per year (i) mean seasonality (j) rainfall onset dates (k) rainfall cessation dates (l) RSL. (1979 – 2018). Black stippling marks significant ($p<0.05$) grid-point trends.

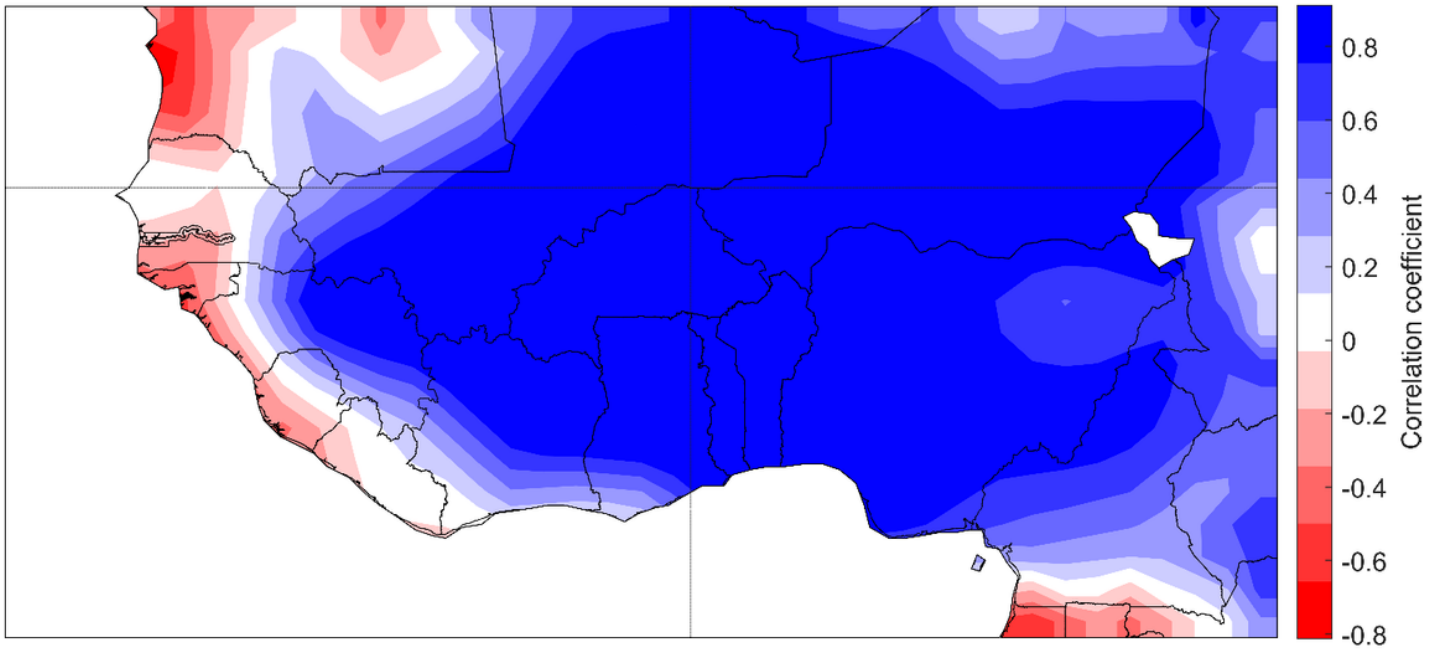

Figure 10

Pearson product-moment correlation between monthly TRMM data (mm/month) and monthly averaged ERA5 precipitation data (mm/month).

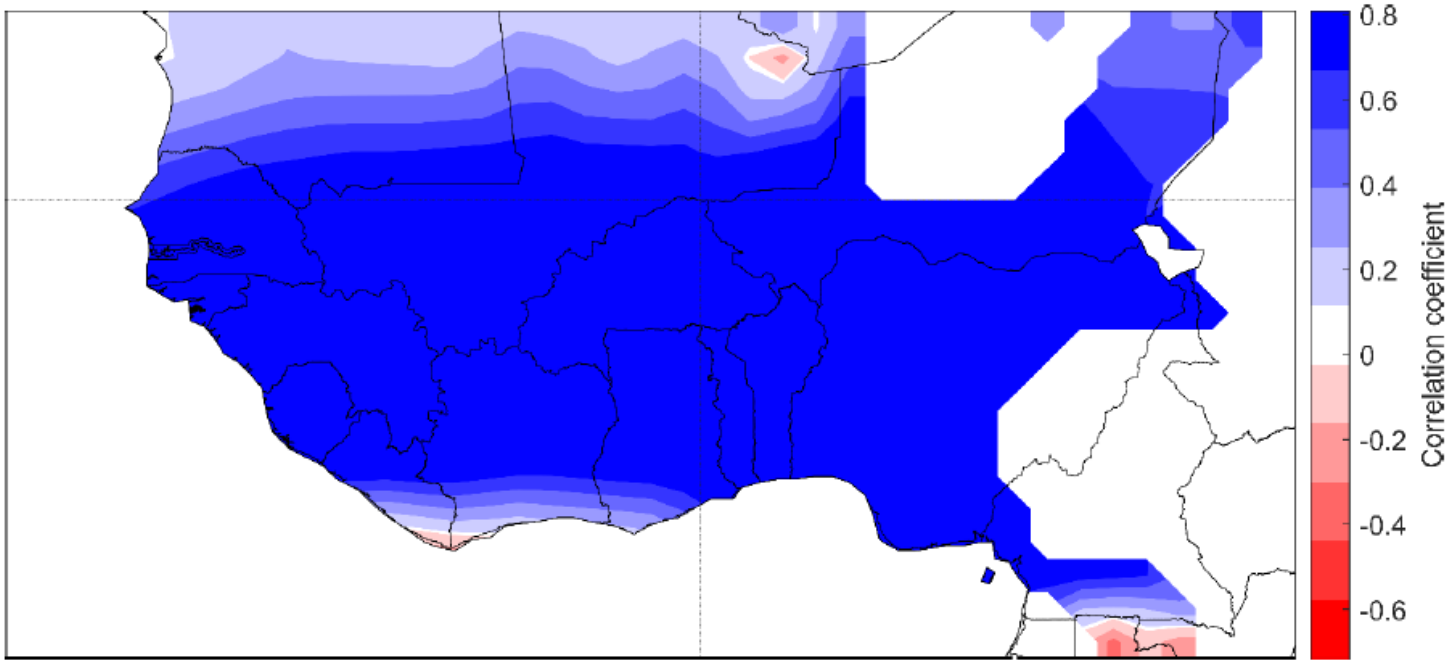

Figure 11

Pearson product-moment correlation between monthly TAMSAT data (mm/month) and monthly averaged ERA5 precipitation data (mm/month). White spaces are missing data in the TAMSAT dataset.

Supplementary Files

This is a list of supplementary files associated with this preprint. Click to download.

- Supplementary.docx